

This article was downloaded by: [Tomsk State University of Control Systems and Radio]

On: 18 February 2013, At: 13:32

Publisher: Taylor & Francis

Informa Ltd Registered in England and Wales Registered Number: 1072954

Registered office: Mortimer House, 37-41 Mortimer Street, London W1T 3JH, UK



## Molecular Crystals and Liquid Crystals Science and Technology. Section A. Molecular Crystals and Liquid Crystals

Publication details, including instructions for authors and subscription information:

<http://www.tandfonline.com/loi/gmcl19>

## Chirality and Frustration in Ordered Fluids

J. W. Goodby<sup>a</sup>, A. J. Slaney<sup>a</sup>, C. J. Booth<sup>a</sup>, I. Nishiyama<sup>a</sup>, J. D. Vuijk<sup>a</sup>, P. Styring<sup>a</sup> & K. J. Toyne<sup>a</sup>

<sup>a</sup> School of Chemistry, The University of Hull, Hull, HU6 7RX, England

Version of record first published: 24 Sep 2006.

To cite this article: J. W. Goodby, A. J. Slaney, C. J. Booth, I. Nishiyama, J. D. Vuijk, P. Styring & K. J. Toyne (1994): Chirality and Frustration in Ordered Fluids, Molecular Crystals and Liquid Crystals Science and Technology. Section A. Molecular Crystals and Liquid Crystals, 243:1, 231-298

To link to this article: <http://dx.doi.org/10.1080/10587259408037771>

PLEASE SCROLL DOWN FOR ARTICLE

Full terms and conditions of use: <http://www.tandfonline.com/page/terms-and-conditions>

This article may be used for research, teaching, and private study purposes. Any substantial or systematic reproduction, redistribution, reselling, loan,

sub-licensing, systematic supply, or distribution in any form to anyone is expressly forbidden.

The publisher does not give any warranty express or implied or make any representation that the contents will be complete or accurate or up to date. The accuracy of any instructions, formulae, and drug doses should be independently verified with primary sources. The publisher shall not be liable for any loss, actions, claims, proceedings, demand, or costs or damages whatsoever or howsoever caused arising directly or indirectly in connection with or arising out of the use of this material.

# Chirality and Frustration in Ordered Fluids

J. W. GOODBY,<sup>†</sup> A. J. SLANEY, C. J. BOOTH, I. NISHIYAMA, J. D. VUIJK,  
P. STYRING, and K. J. TOYNE

*School of Chemistry, The University of Hull, Hull, HU6 7RX, England*

*(Received February 12, 1993)*

Chirality in liquid crystal systems is a complex and sometimes difficult concept to understand and appreciate. In this article we review some of the reduced symmetry aspects of calamitic liquid crystal phases with reference to point symmetry, space symmetry, and helicity. We utilize these concepts in the discussion of new results obtained on Twist Grain Boundary phases, inversions in chiral dependent properties such as the helicity in cholesteric and smectic C\* phases and the spontaneous polarization in ferroelectric liquid crystals, and antiferroelectric behaviour in low molar mass systems. Our observations suggest that many novel effects found in chiral liquid crystals are a result of conflicts between the effects of reduced symmetry and the desire to form normal liquid-crystalline structures, i.e., a form of frustration exists.

*Keywords: liquid crystals, chirality, twist grain boundary phases, inversions, ferroelectrics and antiferroelectrics*

## 1. INTRODUCTION

Chirality in chemical systems has reached a pinnacle of importance in recent years, particularly with the development of new asymmetric reactions which allow chemists to design and create chiral materials almost at will.<sup>1</sup> Nowhere is this success more apparent than in the synthesis of biologically active substances; life, after all, is said to be “handed.” However, the ability to synthesize chiral compounds, with high enantiomeric purities, has also impacted on the development of “advanced materials” through the preparation of novel polymers, liquid crystals, non-linear materials, and compounds used in molecular recognition processes.

In liquid crystal systems the availability of chiral substances of high optical purity has led directly to the discovery of novel phase structures and related phase behaviour. Furthermore, many of the physical properties of chiral liquid-crystalline materials are dependent on the “degree of chirality” exhibited by the material,

<sup>†</sup> Author for correspondence.

which in turn is directly related to enantiomeric excess.<sup>2</sup> For example, liquid crystal phases such as Blue Phases (BPs)<sup>3</sup> and Twist Grain Boundary Phases (TGBPs)<sup>4</sup> have frustrated structures which exist only through the competition between chiral forces and the desire for molecules to pack in ways such that they fill space uniformly. The degree to which these chiral forces/properties are effective is directly related to optical purity.

Chirality in liquid crystal systems, however, encompasses a much wider subject area than just classically defined frustrated phases (e.g. Blue Phases and TGB phases). Topics such as ferroelectric, ferrielectric, and antiferroelectric phases<sup>5</sup>; pyroelectric<sup>6</sup> and piezoelectric properties; non-linear optoelectronic processes; and thermochromism and electrochromism must also be included in the catalogue of chiral effects in ordered fluids. Figure 1 shows a schematic representation of how relationships between chiral liquid crystal phases and symmetry, physical properties, applications and phases structures can be developed and interwoven.

### 1.1. Symmetry in Calamitic Liquid Crystals

In principle, we can define chirality in a number of relatively simple ways<sup>2</sup>; first it can be described by the point symmetry of molecular structure, second through the space symmetry of the structure of the mesophase, and third through the form

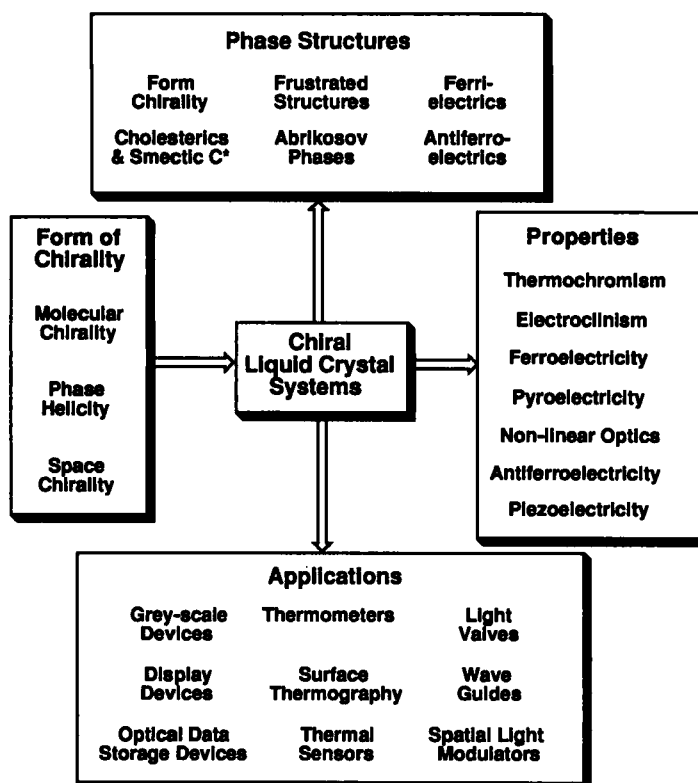


FIGURE 1

chirality of the helical macrostructures of many phases. Point symmetry is itself described by the spatial configuration rules of Cahn, Ingold and Prelog,<sup>7</sup> space symmetry by group theory, and form chirality by helicity or "handedness." Two other important factors that are also coupled to the asymmetry in such systems are the molecular biaxiality and the conformational structure(s) of the molecules.

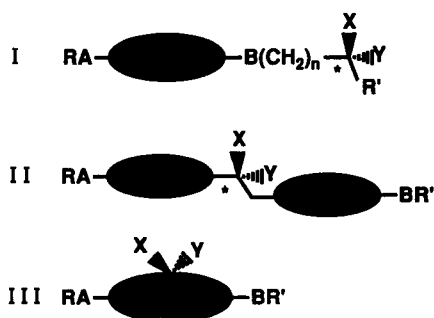
## 1.2. Molecular Symmetry in Smectic Liquid Crystals

Symmetry operations at the molecular level are well-understood and have been carefully defined in recent years. Cahn, Ingold and Prelog<sup>7</sup> have produced an invaluable and universally accepted method of labelling chirality in molecular structures, thereby creating a way of defining the absolute spatial configuration of a molecule. In essence an asymmetric atom can be considered as a point in the molecular structure of a compound that has no mirror symmetry operations associated with it.<sup>8</sup> Thus the (*R*) and (*S*) absolute spatial configuration system defines the local molecular structure about a chiral atom in terms of the atomic numbers of the substituents attached to the asymmetric atom. However, it is important to remember in the case of liquid crystals that this method only defines the spatial configuration conventionally by atomic number and not by any intrinsic molecular property such as polarity or steric shape and size.

Typically there are three ways, as shown in Figure 2, of introducing chiral centres or atoms into, calamitic, rod-like liquid crystals that have two flexible aliphatic chains attached to a rigid aromatic or quasi-rigid alicyclic core.

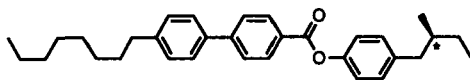
Template structure I (see Figures 2 and 3) is the molecular architecture found in most chiral liquid crystals. The chiral atom is included in the peripheral aliphatic chain, generally because of the ease of synthesis and the availability of suitable chiral substrates, such as alcohols or carboxylic acids.

Type II systems have also been prepared where the chiral centre is in the central region of the molecular structure, however, the bonding structure of asymmetric atoms usually means that the two halves of the molecular core cannot be conjugated with each other. Although liquid crystal phases have been observed in such systems

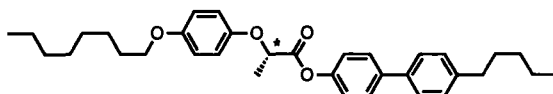


Where A and B are dipolar groups  
X and Y are different atoms or groups,  
and the core is shown as an ellipse

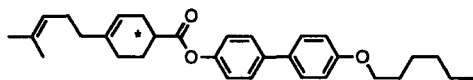
FIGURE 2 Where A and B are dipolar groups X and Y are different atoms or groups, and the core is shown as an ellipse.

**Structure Type I**

Iso - 141 - N\* - 136 - S<sub>A</sub> - 85 - S<sub>C</sub>\* - 69 - S<sub>I</sub>\*  
S<sub>I</sub>\* - 67 - S<sub>F</sub>\* - 66 - J\* - 64 - G\*

**Structure Type II**

M.p. 85, [Iso - (-26) - N\*]

**Structure Type III**

Iso -150 - N\* - 133 - S<sub>A</sub> - 132 - S<sub>C</sub>\*  
S<sub>C</sub>\* - 113 - S<sub>X1</sub> - 94 - S<sub>X2</sub>

FIGURE 3

it is often the case that this structural architecture leads to the destabilization of liquid-crystalline characteristics and the suppression of phase formation.

More recently, attention has focused on attempting to incorporate a chiral centre into the rigid core itself, type III<sup>9</sup> systems. Some chiral alicyclic systems have been prepared that incorporate this design feature. They have been shown to exhibit both chiral nematic and smectic phases. As this statement implies, molecular asymmetry is important in liquid crystal systems because it can impart chirality to the mesophase. This results in the liquid crystal phase having reduced symmetry which leads to helicity and/or ferroelectricity. Examples of the three classes of material typified by the general structures in Figure 2 are given in Figure 3.<sup>10</sup>

The chirality in the above template structures, with respect to the rules of Cahn *et al.*, is determined by the atomic numbers of the substituents X and Y. However, in liquid crystals other aspects of molecular chirality are also important. It is well known, for example, that the steric size and shape of the substituents X and Y and their location with respect to the rigid core are important in determining phase structure type and phase characteristics. The absolute spatial configuration of the chiral atom and its location with respect to the core are often found to determine the handedness of the helix of any helical phase exhibited by the material.

Furthermore optical purity (the relative amounts of the (*R*) and (*S*) enantiomers) is a very important factor in relation to the degree of chirality imparted to the liquid crystal phase. For instance, if the compound is made up of a 1:1 mixture of (*R*) and (*S*) isomers, as in a racemic modification, then the compound will not be

optically active and hence the liquid crystal phase will also be achiral. Consequently, physical properties that are dependent on the chirality of the system will also be dependent on optical purity. Unfortunately, it is often the case that when the physical properties of chiral liquid crystals are evaluated the enantiomeric purity is a neglected property. For instance, when we compare the physical properties of chiral liquid crystals, the results obtained from each individual material should be normalized to take into account the value of the optical purity. Thus, when a material is composed of an ideally compensated mixture of enantiomers the magnitude of a property such as the spontaneous polarization will be zero, whereas the highest value attainable should be for an enantiomeric excess of 1. Linear relationships between enantiomeric excess and the physical properties dependent on the chirality of a material are expected, but have not yet been experimentally verified.

### 1.3. Space Symmetry

In certain liquid crystal phases the space symmetry also has to be taken into account, in particular this applies to the ferroelectric smectic  $C^*$  phase,<sup>11</sup> its related anti- and ferroelectric states, and related crystal phases  $G^*$ ,  $H^*$ ,  $J^*$ , and  $K^*$ , and to electroclinicism<sup>12</sup> in the orthogonal smectic phases,  $A^*$ ,  $B^*$ , and  $E^*$ .<sup>13</sup> It is difficult to define symmetry operations in fluid phases where the molecules are undergoing rapid changes in conformational structures, and therefore, we can only consider the simple situation of the local or environmental symmetry in the mesophase, say for a small molecular ensemble, and then apply this to the bulk phase. For example, consider the structure of the smectic  $C$  phase, when it is composed of achiral molecules or a racemic modification then the environmental or local space symmetry consists of a centre of inversion, a mirror plane normal to the layers, and a  $C_2$  axis parallel to the layers and normal to the tilt direction. Thus, the symmetry can be described as  $C_{2h}$ . However, when the molecules of the phase are optically active the local symmetry in the layers is reduced to a polar  $C_2$  axis. As the molecules are themselves polar, there is an inequivalence with respect to the dipoles along the  $C_2$  axis. This inequivalence occurs even though the molecules are undergoing rapid reorientation motion about their long axes. The time dependent alignment of the dipoles along the  $C_2$  axis causes a spontaneous polarization to develop along this direction, parallel to the layer planes and perpendicular to the tilt direction of the molecular long axes, as shown in Figure 4. As a consequence each individual layer can be considered as having a spontaneous polarization, and because the phase has  $C_2$  symmetry the polarization must be directional ( $Ps(+)$  or  $Ps(-)$ ).

### 1.4. Helical Structures in Smectic Liquid Crystals

When certain liquid crystal phases are composed of chiral material they will also exhibit helical macrostructures. In the chiral nematic phase a helix is formed by a rotation in the packing of the molecules perpendicular to their long axes. The rotation direction has the same sense throughout the phase, and hence a twist forms perpendicular to the director of the phase. In Blue Phases a similar arrangement exists but this time the twist can occur in more than one direction resulting in the formation of a frustrated structure.<sup>3</sup>

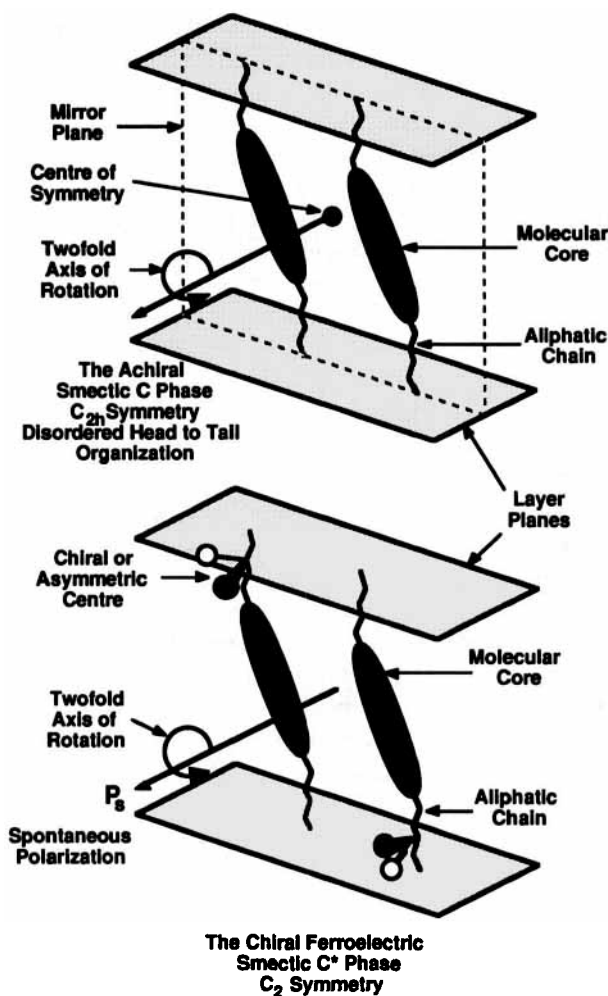


FIGURE 4 The direction of the polarization in the lower figure is defined as  $Ps(-)$ .

In the smectic phases C, I, and F phases the long axes of the molecules are tilted with respect to the layer planes of the phase. When any of these phases incorporate optically active materials in their structures the phase becomes helical. Thus, for a single component material, a spontaneous temperature-dependent twist of the tilt orientation is induced about an axis normal to the layers. Thus, there is an angle (azimuthal angle,  $\phi$ ) between the plane containing the layer normal and the director for adjacent layers, and as this rotation is always in the same direction a helical macrostructure is formed. The twist can be either right- or left-handed, and as the pitch of the helix formed is temperature-dependent, the phase will selectively reflect light when the pitch is comparable to the wavelength of light, hence the phase becomes iridescent. For the more ordered chiral crystal phases,  $G^*$ ,  $H^*$ ,  $J^*$ , and  $K^*$ , the three dimensional long range periodic ordering of the molecules effectively suppresses the formation of a helical structure.



In the antiferroelectric phase a slightly different variation on the helical structure of the smectic C\* phase is found. In the unwound (non-helical) structure of the antiferroelectric phase, molecules in adjacent layers are tilted in opposite directions to one another, as if adjacent layers had been rotated by 180° with respect to each other. In the helical case, the zigzag bilayer structure is rotated in one preferred direction about the direction normal to the layers. Furthermore, the zigzag local ordering of the molecules causes a repeat in the helical structure for a 180° rotation about the helical axis, as shown in Figure 5.

The Twist Grain Boundary phase also exhibits a macroscopic helical structure, but as this novel phase is the subject of a later part of this article its structure will not be discussed in depth here, save to say that it is caused by a competition between the desire for the molecules to form a layered structure as in a normal smectic phase, and the tendency for the molecules to pack together to form a helical structure as in a chiral nematic phase.

### 1.5. Combined Effects of Reduced Symmetry

The smectic C\* phase can be used as an example of a liquid crystal phase that displays the three types of chirality given above. Firstly the constituent molecules of the phase are chiral and therefore possess point symmetry in relation to their asymmetric centres, secondly when packed in layers where the molecular long axes are tilted with respect to the layer planes, the phase has C<sub>2</sub> space symmetry, and thirdly the stacking of the layers one on top of another results in the tilt precessing about the normal to the layers creating a macroscopic helical structure<sup>14</sup> as shown in Figure 6.

### 1.6. Structures of Chiral Liquid Crystal Phases

The structures of chiral mesophases are many and varied. In all cases a material that exhibits a chiral mesophase must be optically active (even for a mixture of compounds), and as a consequence all of the phases will have chiral space symmetries, but, not all are required to exhibit helical macrostructures. Thus, helicity is a secondary structural property, which can be suppressed without change to the molecular or space asymmetry. Typically, the structures of chiral mesophases of calamitic materials fall into five categories, frustrated phases, orthogonal phases, tilted phases, cholesteric phases, and quasi-crystalline phases.<sup>15</sup> In all, but the orthogonal and quasi-crystal phases, helical macrostructures are observed. Figure 7 shows a schematic representation of the structures of some chiral mesophases.

### 1.7. Rotational and Conformational Order in Chiral Liquid Crystals

In the case of the structures of the cholesteric and blue phases the molecules are orientationally ordered, but at the same time they are rotationally disordered with respect to their long axes. Similarly, in the smectic state the molecules are orientationally ordered, but unlike the cholesteric and Blue phases the molecules packed in diffuse, poorly structured layers. Again the molecules are rotationally disordered with respect to their long axes, and there is no long range positional order within or between the layers. Only in the quasi-crystalline smectic phases do the molecules

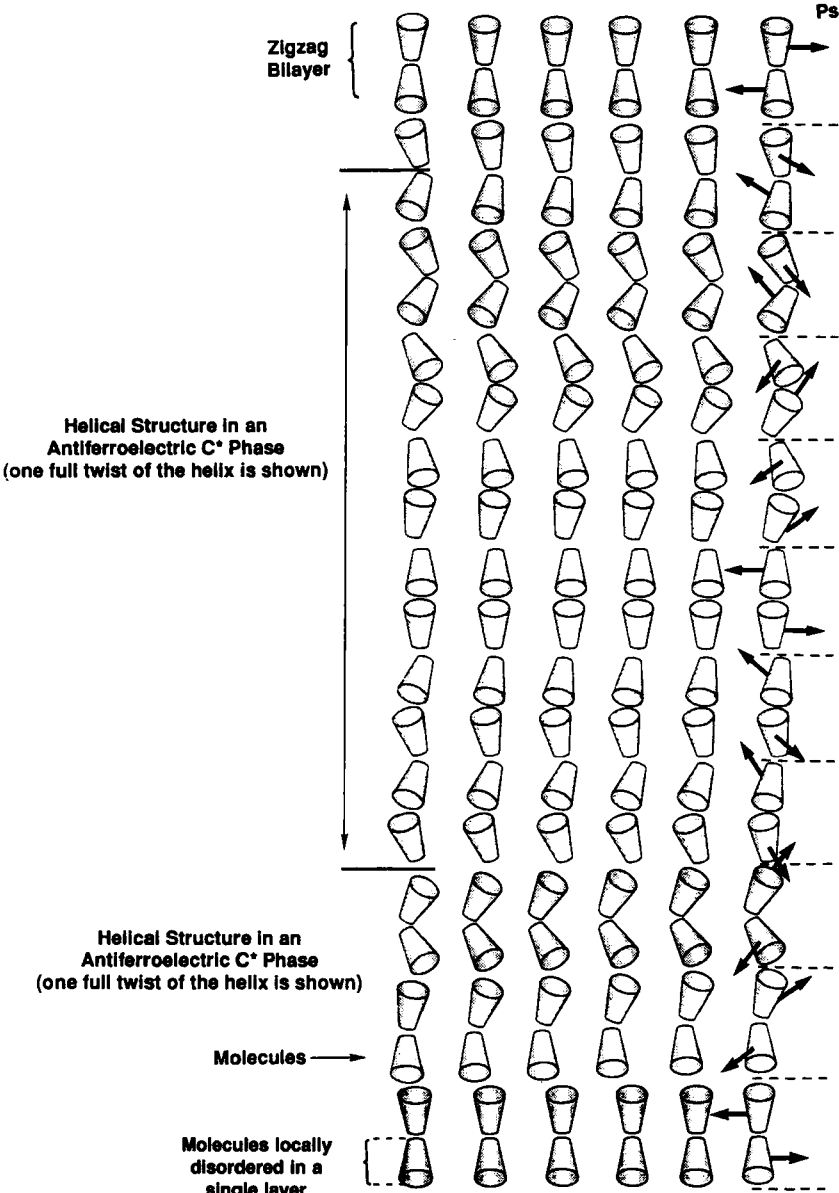


FIGURE 5 The proposed helical structure of the antiferroelectric smectic C\* phase.

have long range periodic ordering, but like the other phases the constituent molecules are rotationally disordered. In this brief analysis of the structures of chiral calamitic mesophases it is important to note that in each case, the rotational disorder can affect the chiral interactions of the molecules considerably, thereby in turn affecting chirality dependent liquid-crystalline properties. For example, the helical pitch length in cholesteric and smectic C\* phases, the magnitude of the spontaneous polarization and second harmonic generation (SHG) efficiencies<sup>16</sup> in ferroelectric

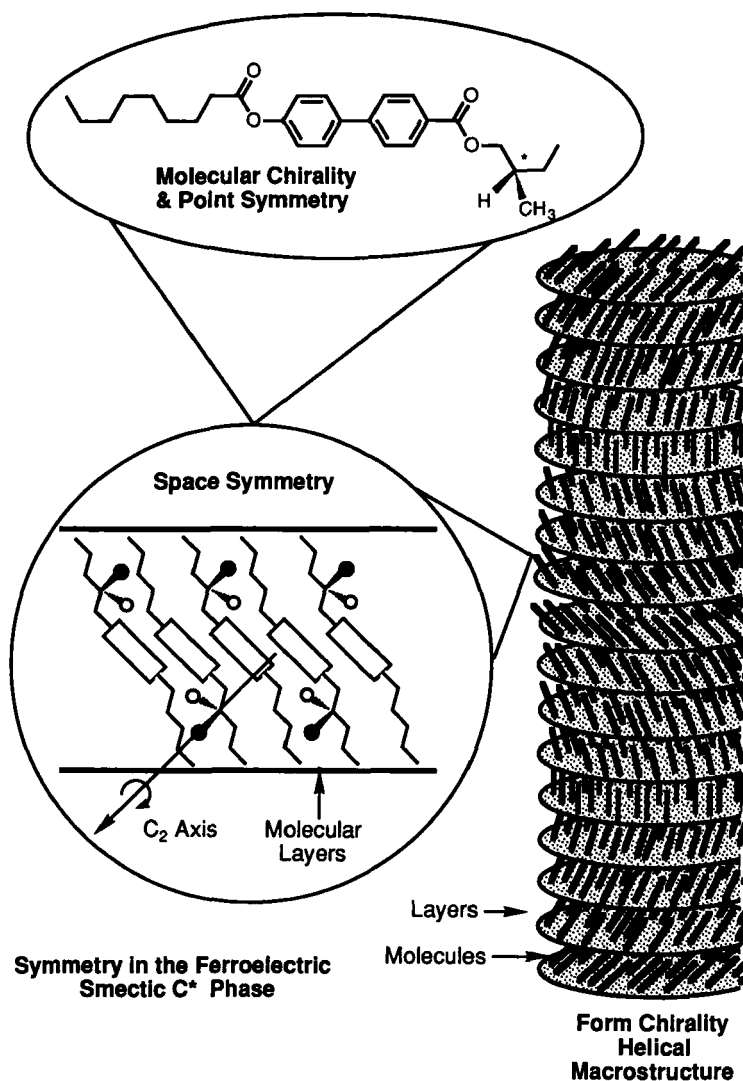


FIGURE 6

phases, and phase transition temperatures can be markedly affected by the rotational disorder of the molecules. The rotational disorder can take two forms, that of the molecule as a whole about its long axis, which is related to the biaxiality of the system, and the internal rotational disorder which is related to the conformational structures of the molecules making up the mesophase.

For example, consider the problem of designing and synthesizing a material that exhibits a ferroelectric smectic C\* phase which has a relatively large spontaneous polarization. First, it is important to understand the origin of the polarization at a molecular level.<sup>17</sup> For this purpose, it is useful to consider a relatively simple model for a molecule in the smectic C\* phase, as shown in Figure 8. In this figure the molecule is shown as a simple rod which is tilted at an angle of  $\theta$  to the layer planes,

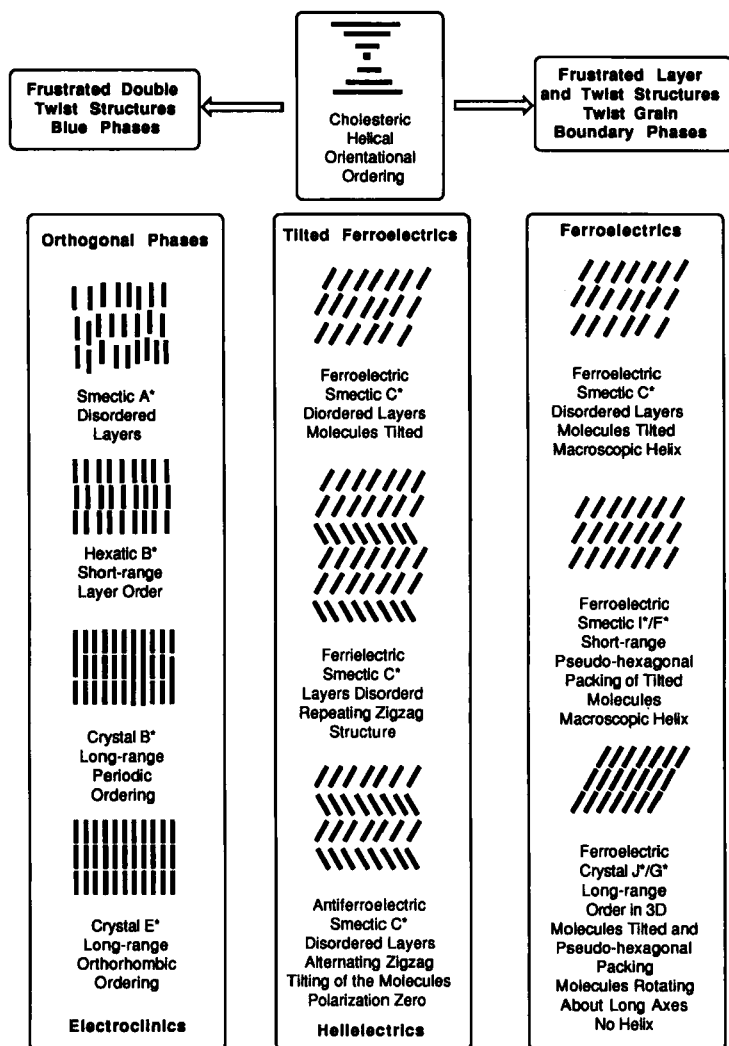


FIGURE 7 Structures of some chiral liquid crystal phases, the molecules are shown as rods.

thus rotation of the molecule over a surface of constant energy, about the tilt angle, sweeps out a cone of revolution that has an angle at its apex of  $2\theta$ . We also need to assume that the molecule has a lateral dipole,  $\mu_r$ , perpendicular to its long axis, and that the dipole is positioned at an angle of  $\Psi$  to the  $C_2$  axis of the phase.

If we now consider the energy diagram showing potential energy as a function of the angle,  $\Psi$ , between the transverse dipole moment of the molecule,  $\mu_r$ , and the  $C_2$  axis, we find that, the magnitude of the polarization will depend on the depth and shape of the energy curve. If the molecule has no chiral centre, the energy at  $\Psi = 0^\circ$  and  $180^\circ$  should be same, as shown in Figure 9(a). Furthermore, there is no net polarization as a whole, even though  $\mu_r$  may still exist along the direction of the  $C_2$  axis. The introduction of the chiral centre into the molecular structure breaks the symmetry and creates an energy difference ( $\Delta E$ ) between the

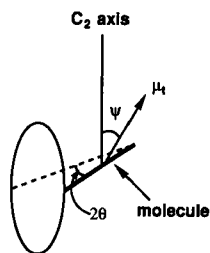


FIGURE 8 A simple model for the local structure associated with one molecule in the smectic  $C^*$  phase,  $\mu_t$  is the transverse dipole moment of a molecule,  $\Psi$  is the angle between  $\mu_t$  and  $C_2$  axis, and  $\theta$  is the tilt angle.

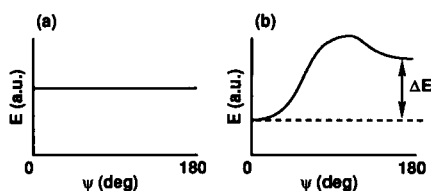


FIGURE 9 The effect of the introduction of a chiral centre on the shape of the energy diagram in the  $C$  phase. (a) For an achiral molecule, there is no energy difference between  $\Psi = 0^\circ$  and  $180^\circ$ . (b) The introduction of a chiral centre into the structure of the molecule breaks the symmetry along the  $C_2$  axis creating an energy difference,  $\Delta E$ , between the two positions.

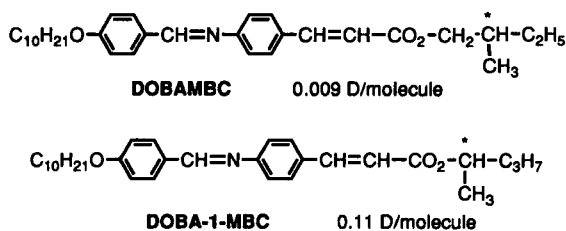


FIGURE 10 Comparison of the molecular polarization in two isomeric compounds.

positions at  $\Psi = 0^\circ$  and  $180^\circ$ , see Figure 9(b) (the shapes of the energy curves for both diagrams are shown schematically), and this consequently produces a polarization along the direction where  $\Psi = 0^\circ$  as shown in Figure 9(b).

Thus, as the energy difference,  $\Delta E$ , results from a reduction in symmetry caused by the introduction of a chiral centre, one obvious way to increase the size of  $\Delta E$  is to bring the dipole and the chiral centre close together. This has the effect of increasing the coupling between the lateral dipole and the part of the molecular structure involved in the symmetry breaking operation. For example, replacement of the 2-methylbutyl chiral unit of DOBAMBC by the isomeric 1-methylbutyl unit (DOBA-1-MBC)<sup>18</sup> increases the polarization by more than a factor of 10 (see Figure 10).<sup>19</sup>

Another way to increase the value of  $\Delta E$  is to restrict the rotation of the chiral centre (not that of the dipole) thereby increasing the degree of coupling of the lateral dipole with the source of the chirality. For instance, if the chiral centre is allowed to rotate freely and homogeneously about the director, then there will be no energy difference for any value of  $\Psi$ . One way of restricting the rotation of the chiral moiety is to extend the terminal aliphatic chain on the peripheral side of the chiral centre, thereby burying the chiral centre in the structure of the molecule.<sup>20</sup> It is important to note that positions along the terminal chain closer to the centre of the molecule will have less mobility associated with them.

Results from earlier research, on the effect that changing the alkyl chain length on the external side of the chiral centre has on the magnitude of the polarization, confirm the above postulation. For example, the value of the spontaneous polarization was determined for compounds DOBA-1-MBC and DOBA-1-MPC, the results found are shown in Figure 11.<sup>18</sup>

Thus, extension of the peripheral aliphatic chain appended to the chiral centre of DOBA-1-MPC by one methylene unit (i.e., to give DOBA-1-MBC) was found to almost treble the value of the spontaneous polarization even though the dilution effect caused by increasing the volume size of the molecule should have reduced the overall value.

Similarly, we found analogous results via the synthesis of a number of (*R*)- and (*S*)-1-methylalkyl 4-(*n*-octanoyloxy)biphenyl-4'-carboxylates. This investigation sought to study systematically the effect of damping of the motion of the chiral centre on the magnitude of the spontaneous polarization. As with study of the analogues of DOBAMBC, it was found that damping of the motion of the chiral centre substantially increases the value of the spontaneous polarization, as shown in Table I.

Finally, it should be noted that in the case where two materials have the same energy difference,  $\Delta E$ , in the energy diagram, it is probable that they will still have different polarization values. This is because the magnitude of the spontaneous polarization is also dependent on the shape of the energy diagram. A compound having an energy diagram as shown in Figure 12(a) would possess a larger polarization value than the compound possessing an energy diagram of the form shown in Figure 12(b). For instance, the dipole moment projected on to the  $C_2$  axis ( $\Psi = 0^\circ$ ) would have to be larger in the case of 12(a) with respect to that for 12(b). This could be realized by increasing the rotational hindrance of the dipole, thereby increasing the effective dipole projected along the  $C_2$  axis.

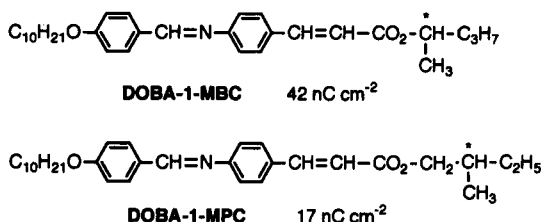


FIGURE 11 Comparison of the spontaneous polarization. The values were determined at  $T_{AC} - T = 5^\circ\text{C}$ .<sup>18</sup>

TABLE I

Effect of alkyl chain length on the absolute polarization ( $P_o$ )<sup>20</sup>

$\text{C}_8\text{H}_{17}\text{COO}-\text{C}_6\text{H}_4-\text{C}_6\text{H}_4-\text{COO}-\overset{*}{\underset{\text{CH}_3}{\text{CH}}}-\text{C}_n\text{H}_{2n+1}$	
n	$P_o$ (nC cm <sup>-2</sup> °C <sup>-α</sup> )
2	7.7
3	32.0
4	30.7
5	48.8
6	42.2

Thus, in principle point symmetry and phase symmetry affect the overall chirality of the system, but we still have to take into account molecular structure, conformational structure, and rotational disorder when we appraise the overall effect of chirality. As noted above, rotational freedom can markedly affect matters, and in Figure 13 we attempt to show how certain intramolecular interactions can affect this process. In the following sections we discuss this matter from a practical standpoint through the synthesis of materials, where the steric shape of the molecule has been designed to investigate these effects further and to explore the extremes of the effects of chirality in liquid crystal systems.

Thus, in this section of the introduction we draw attention to the fact that the chirality of a liquid crystal system is affected usually, but not always, by three symmetry considerations; point, space, and form symmetry. In turn the degree of chirality is affected by optical purity, biaxiality, rotational hindrance, dipole size, steric shape, and conformational structure. Consequently, the topic of chirality is a very complex one, and as it is difficult to cover all aspects of the subject in one article, only the following topics will be discussed in more detail with reference to the symmetry and rotational hindrance arguments described above:

- (a) frustration and Twist Grain Boundary phases,
- (b) inversions in chiral properties, and
- (c) antiferroelectric effects in smectic phases.

Blue Phases, cholesterics, and ferroelectrics will not be dealt with in any depth as they will be discussed elsewhere.

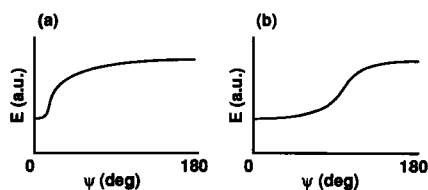


FIGURE 12 Effect of restriction of the dipole on the shape of the energy diagram. If the dipole is restricted, the energy curve would steepen about the energy minimum, as shown in (a).

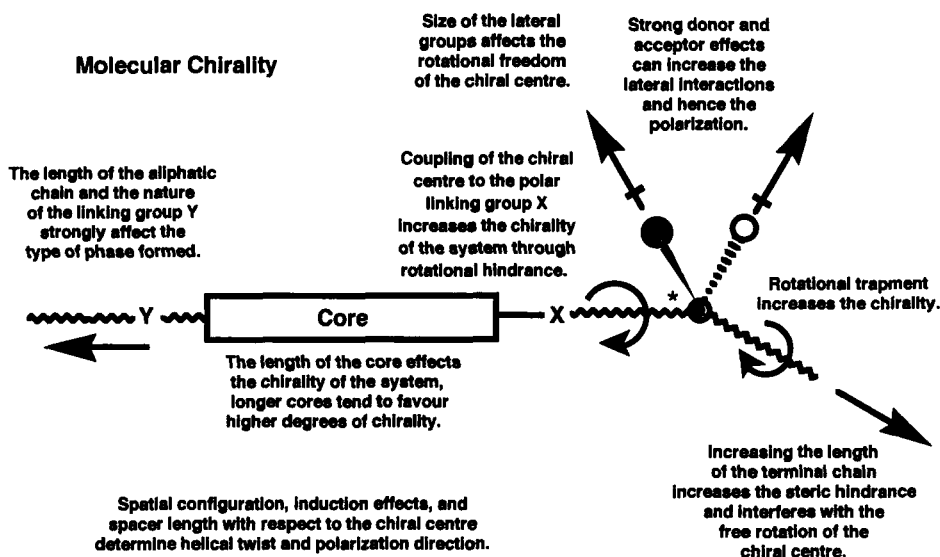


FIGURE 13

## 2. FRUSTRATED PHASES AND TWIST GRAIN BOUNDARY PHASES

Twist Grain Boundary (TGB) phases are typically detected at the phase transition from the liquid or cholesteric states to the smectic state.<sup>21</sup> So far stable Twist Grain Boundary phases have been found to mediate the cholesteric to smectic A\*, isotropic liquid to smectic A\*, and cholesteric to smectic C\* transitions. This gives rise to corresponding TGB<sub>A\*</sub> and TGB<sub>C\*</sub> phases which generally exist over a temperature range of a few degrees.

### 2.1. The de Gennes' Analogy with Superconductors

The presence, and to some degree the discovery, of TGB phases in liquid-crystalline systems stems from theoretical studies made by de Gennes.<sup>22</sup> Through his modeling of the N—A transition de Gennes predicted that, for a second order nematic to smectic A phase transition, a defect stabilized phase could occur when the liquid crystal was subjected to twist or bend distortions. Furthermore, de Gennes also sought to unify his physical theory of the nature of this phase transition with similar theories for phase transitions in superconductors. In his analogy, de Gennes suggested that the twist and bend distortions could be incorporated into a layered smectic A structure via the presence of an array of screw or edge dislocations. The screw dislocations permeate the normal A phase in the form of a lattice, and this is similar to how the conducting phase permeates the superconducting phase to form a lattice of vortices in the Abrikosov flux phase of Type II superconductors.<sup>23</sup> Relationships between liquid crystals and superconductors in the de Gennes analogy are summarised in Table II.

This analogy was further developed by Renn and Lubensky<sup>4</sup> to incorporate chiral systems. In their theoretical modeling it was suggested that a similar intermediary



TABLE II

The analogy between superconductors and liquid crystals (after Renn and Lubensky)

Superconductor	Liquid Crystal
$\psi$ = Cooper pair amplitude	$\psi$ = density wave amplitude
$A$ = vector potential	$n$ = nematic director
$B = \nabla \times A$ = magnetic induction	$\kappa_0 = n \cdot \nabla \times n$ = twist
normal metal	nematic phase
normal metal in a magnetic field	cholesteric ( $N^*$ ) phase
Meissner phase	smectic A phase
Meissner effect	twist expulsion
London penetration depth $\lambda$	twist penetration depth $\lambda_t$
superconducting coherence length $\xi$	smectic correlation length $\xi$
vortex (magnetic flux tube)	screw dislocation
Abrikosov flux lattice	twist grain boundary phase

phase could also be formed at the cholesteric to smectic  $A^*$  transition. This phase was predicted to be stabilized by a lattice of screw dislocations, which they expected to form in rows or chains, and hence they named the phase the Twist Grain Boundary Phase ( $TGB_A$ ). Subsequently, they developed their models further to incorporate the cholesteric to smectic  $C^*$  transition; the phase predicted to be formed in this case was called the  $TGB_C$  phase. Two forms of this phase are expected, one where the molecules are simply inclined to the layer planes with no interlayer twist, and another where they are allowed to form helical structures normal to the layer planes in addition to the helices formed by the screw dislocations.<sup>24</sup>

Thus, at a normal cholesteric to smectic  $A^*$  transition, the helical ordering of the cholesteric phase collapses to give the layered structure of the smectic  $A^*$  phase. However, for a transition mediated by a TGB phase, there is a competition between the need for the molecules to form a helical structure due to their chiral packing requirements and the need for the phase to form a layered structure. Consequently, the molecules relieve this frustration by trying to form a helical structure, where the axis of the helix is perpendicular to the long axes of the molecules (as in the cholesteric phase), yet at the same time they also try to form a lamellar structure as shown in Figure 14. These two structures are incompatible with one another and cannot co-exist and still fill space uniformly without forming defects. The matter is resolved by the formation of a periodic ordering of screw dislocations which enables a quasi-helical structure to co-exist with a layered structure. This is achieved by having small blocks of molecules, which have a local smectic A structure, being rotated with respect to one another by the screw dislocations, thereby forming a helical structure.<sup>25</sup> As the macroscopic helix is formed with the aid of screw dislocations, the dislocations themselves must be periodic. It is predicted that rows of screw dislocations in the lattice will form grain boundaries in the phase, and hence the new phase was referred to as the twist grain boundary (TGB) phase.

In this analysis it must be emphasized that the TGB phase is not simply a layered

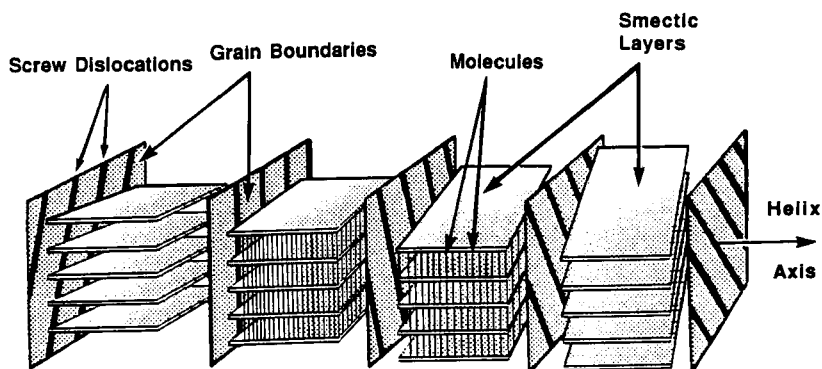
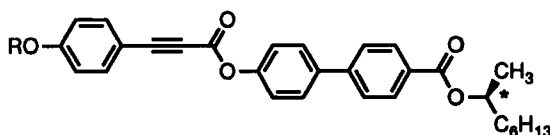
FIGURE 14 Structure of the Abrikosov  $TGB_A$  Phase.

FIGURE 15

cholesteric phase, and should not be confused with this concept. A layered cholesteric phase simply cannot exist on a macroscopic scale, and it is a requirement that defects must be formed.

## 2.2. TGB Materials

Examples of this theoretically predicted phase were first discovered in some propiolate esters of “high liquid-crystalline chirality,” shown in Figure 15.

These materials<sup>26</sup> were synthesized so as to have high optical purities, their chiral centres were located adjacent to the rigid molecular cores in order to couple strongly with the dipolar regions of the cores, and the peripheral terminal chains appended to the external sides of the chiral centres were made to be relatively long so as to increase the rotational steric hindrance. Certain members of this family of materials were found to exhibit exotic phase behaviour in that they formed the Twist Grain Boundary phase directly on cooling from the isotropic liquid. The helical structure in the  $TGB_A$  phase of these materials appears, from experimental studies, to have a pitch length in the range of 0.38 to 0.63 micrometers; therefore the phase, like the cholesteric phase, selectively reflects light. Studies appear to indicate that the block size is about 185 Å, which is quite small considering that the phase is still smectic.<sup>25</sup> Verification of the presence of a lattice of screw dislocations was found to be difficult to obtain through x-ray diffraction experiments, however, freeze-fracture studies have been instrumental in confirming the structure of the  $TGB_A$  phase.<sup>27</sup> Thus, these remarkable phases and phase transitions can be said to be the result of the competition between chirality and conventional phase structure.

Since the discovery of the first TGB materials in 1989 a wider range of materials that exhibit this phase have been discovered.<sup>28</sup> Generally they all tend to have

similar structures to the original TGB compounds. A list of homologous series of compounds for which some members exhibit TGB phases is given in Figure 16. This compilation is by no means complete as many individual compounds also possess TGB phases, however, this growing list is now so long that single materials are not given here. It is also interesting to note that the benzoate esters, analogous in structure to the phenylpropiolates (the original TGB materials), do not readily exhibit TGB phases with fewer compounds in the series showing such properties.

“Abrikosov-like” phases are also believed to be exhibited by some optically active side-chain liquid crystal polymethacrylates, where the mesogenic side-group

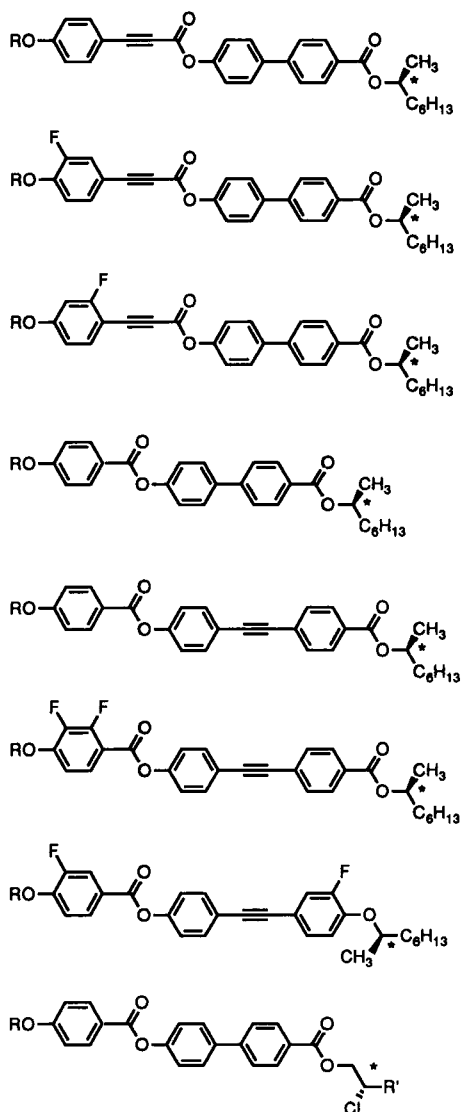


FIGURE 16 Structures of homologous series of compounds where some members exhibit TGB phases.<sup>29</sup>

is derived from cholesterol.<sup>30</sup> The polymer, of structure shown below in Figure 17, was reported to exhibit a twisted layered structure in its smectic A phase, and the authors likened this to a layered cholesteric phase. Clearly such a structure cannot exist without the creation of defects and hence the ensuing formation of a lattice defect structure. Thus, presumably this polymer must also exhibit a Twist Grain Boundary phase like low molar mass materials. Possibly, as the liquid crystal phase develops from either the liquid or the crystal states, the main chain of the polymer prevents a cholesteric phase from forming and instead induces the formation of a smectic A phase. However, the strong chirality of the side group in turn forces the layers to twist to give an "Abrikosov phase."

Work on non-steroid systems also reveals that TGB phases can also be formed in more conventional chiral polymers. Figure 18 shows the structure of another polymethacrylate which exhibits cholesteric, TGB<sub>A</sub>\*, smectic A\*, and ferroelectric smectic C\* phases.<sup>31</sup> It is interesting to note that the directly analogous polyacrylate<sup>32</sup> does not possess such disordered phases and therefore does not exhibit a TGB phase.

### 2.3. The 1-Methylheptyl 4'-(4"-*n*-Alkoxyphenylpropioloyloxy)biphenyl-4-carboxylates

The first twist grain boundary phases discovered in low molar mass materials were found in the optically active variants of the 1-methylheptyl 4'-(4"-*n*-alkoxyphenyl-

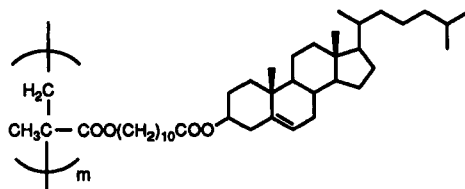
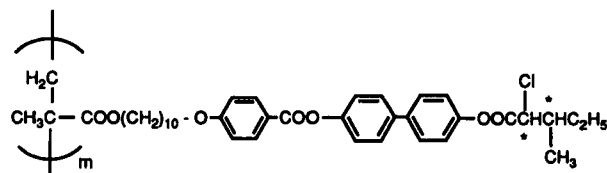
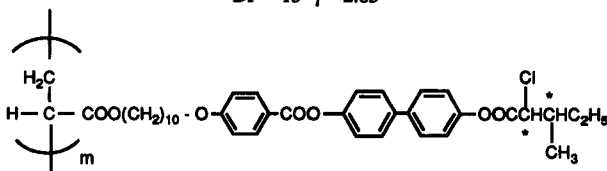


FIGURE 17



Iso 160 N\* 149 TGB<sub>A</sub>\* 140 S<sub>A</sub>\* 73 S<sub>C</sub>\*

DP = 15  $\gamma$  = 2.65



Iso 194 S<sub>A</sub>\* 152 S<sub>C</sub>\* 109 S<sub>2</sub> 75 S<sub>1</sub>

DP = 12  $\gamma$  = 1.32

FIGURE 18

ylpropioloyloxy)biphenyl-4-carboxylates (1M7nOPBBCs).<sup>26</sup> The general chemical structure for this family is shown earlier in Figure 15.

The phase transitions for this series were examined and determined by thermal optical microscopy and differential scanning calorimetry, the results for which are given in Table III. The transition temperatures (°C) for the series are plotted as a function of increasing *n*-alkoxy chain length in Figure 19. It can be seen that, as the series is ascended, the smectic A\* to smectic C\* transition temperatures rise sharply. Over the same interval of chain length the smectic A\* to isotropic liquid transition temperatures fall, thereby decreasing the temperature range of the smectic A\* phase with increasing chain length. For the hexadecyloxy homologue this effect results in a direct smectic C\* to isotropic liquid transition. Thus, the smectic A\* phase senses an increasing degree of fluctuations from both the isotropic liquid and the smectic C\* phase as the series is ascended.<sup>22</sup> If we now examine the variation

TABLE III

Transition temperatures (°C) and clearing point enthalpies (cal g<sup>-1</sup>) for the (*R*)- and (*S*)-1-methylheptyl 4'-(4''-*n*-alkoxyphenylpropioloyloxy)biphenyl-4-carboxylates (1M7nOPBBCs)

<i>n</i>	Iso to A* or TGBA*	Iso to C*	A* or TGBA* to C* †	C* to C*ferri †	C*ferri to C*anti †	mp	Recryst
8	97.5					81.3	58.5
ΔH	1.6					11.3	
9	97.5					81.3	58.4
ΔH	1.4					12.1	
10	98.0		[76.3]			85.4	76.8
ΔH	1.5					12.3	
11	95.0		[78.1]	[56.0]	[44.6]	85.1	75.9
ΔH	0.8					12.8	
12	96.3		86.0	[57.3]	[48.0]	82.4	36.4
ΔH	0.9					11.4	
13	94.1		88.3	[57.1]	[43.7]	81.6	33.7
ΔH	0.5					10.8	
14	93.8		89.7	[53.4]	[42.5]	78.3	37.2
ΔH	0.3					11.0	
15	91.6		90.6	(50.0)		76.5	52.0
ΔH	0.2					11.4	
16		99.0				73.4	25.6
ΔH		0.4				10.5	

Where [ ] denotes a monotropic transition,

( ) denotes a virtual transition (observed on fast supercooling),

† denotes a phase transition where the enthalpy was too small to be measured.

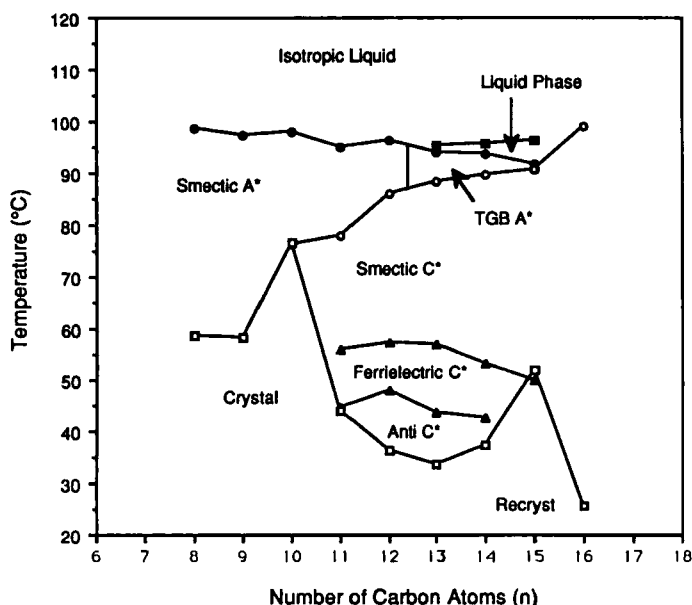


FIGURE 19 Transition temperatures ( $^{\circ}\text{C}$ ) shown as a function of  $n$ -alkoxy chain length for the ( $R$ )- and ( $S$ )-1-methylheptyl 4'-(4''- $n$ -alkoxyphenylpropionyloxy)biphenyl-4-carboxylates (1M7nOPPBCs). The melting points are omitted from the figure for reasons of clarity.

in the clearing point enthalpy with respect to chain length we find that the values fall sharply as the  $n$ -alkoxy chain length is increased. Thus, the clearing point transitions appear to become more weakly first order in nature with increasing  $n$ -alkoxy chain length.

The sharp decrease in enthalpy values for the clearing points (as shown in Figure 20) coupled with the decreasing smectic  $A^*$  range on ascending the series appear to satisfy the criteria set out by de Gennes<sup>22</sup> for the emergence of dislocation stabilized phases, i.e., the transitions should become more second order in nature and strong pretransitional effects must be felt for defect stabilized phases to occur. Hence the tridecyl to pentadecyl homologues were found to exhibit Twist Grain Boundary ( $\text{TGB}_{A^*}$ ) phases because the projected temperature ranges of their smectic  $A^*$  phases were relatively short. Figure 20 shows how the clearing point enthalpies fall dramatically with increasing chain length, and it is interesting to note the sudden increase in value for the  $n$ -hexadecyloxy homologue which exhibits a direct isotropic to smectic  $C^*$  transition, i.e., the clearing point transition appears to be becoming more strongly first order again as the smectic  $C^*$  modification becomes the dominant phase.

These studies also show two other interesting effects, firstly certain members in the homologous series exhibit ferrielectric and antiferroelectric phases, and secondly for the materials that exhibit  $\text{TGB}_{A^*}$  phases, a novel transition is found to occur in the isotropic liquid.

The ferri- and anti-ferroelectric phases appear first for the undecyl homologue on ascending the series, and disappear once the chain length reaches sixteen carbon

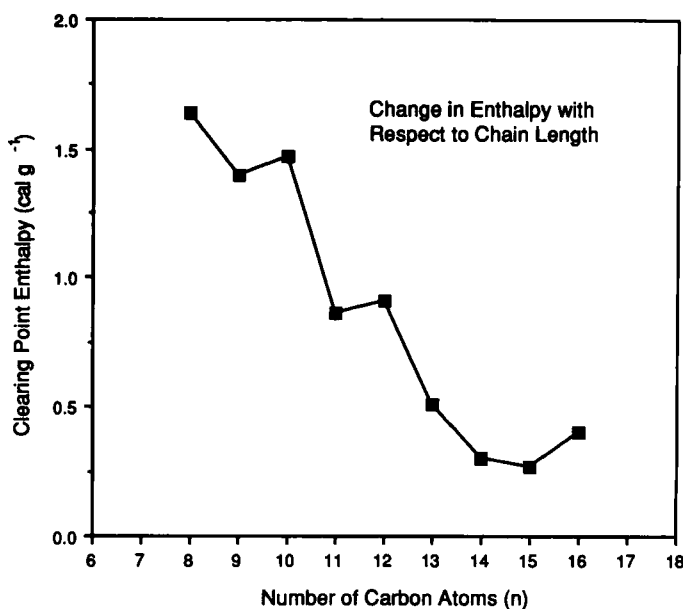


FIGURE 20 Transition temperatures ( $^{\circ}\text{C}$ ) shown as a function of  $n$ -alkoxy chain length for the ( $R$ )- and ( $S$ )-1-methylheptyl 4'-(4'- $n$ -alkoxyphenylpropionyloxy)biphenyl-4-carboxylates (1M7nOPPBCs).

atoms in length. A later section in this article will deal in more detail with these phases so they will not be discussed further here.

Above the clearing point transitions the materials also exhibit enthalpies in the temperature range of the isotropic liquid. These transitions are detected as broad diffuse peaks by differential scanning calorimetry in both heating and cooling cycles. No effects are observed in the polarizing microscope for this transition however, suggesting that the two liquid states have very similar properties and any ordering of the molecules in the lower temperature liquid phase must be weak. The presence of this new liquid phase has been verified by x-ray diffraction and polarimetry studies. It is interesting to note that when these materials are prepared in their racemic forms this liquid-liquid phase transition disappears. Moreover, the clearing temperature moves to a higher value and the magnitude of the associated enthalpy also increases. For each of the homologues that exhibit TGB phases, if the clearing point enthalpy for the liquid to TGB phase transition is added to the value for the liquid to liquid transition, then the total value is approximately equal to that for the smectic A to isotropic transitions in the equivalent racemate. This is further evidence to support the view that the liquid to liquid transition is real and not an artifact.

It is also interesting that the clearing point temperatures are lower for the optically active compounds in comparison to their racemic equivalents (by almost  $4^{\circ}\text{C}$  for the tetradecyloxy homologue) which is in agreement with de Gennes' theoretical model. These results clearly show that chirality and optical purity can markedly affect transition temperatures in liquid crystal systems. Table IV gives the liquid to liquid transition temperatures for the  $\text{C}_{13}$  to  $\text{C}_{15}$  homologues and related values for the racemic form of the tetradecyloxy homologue.

TABLE IV

Transition temperatures ( $^{\circ}\text{C}$ ) and enthalpies ( $\text{cal g}^{-1}$ ) for the (*R*), (*S*), and racemic forms of the 1-methylheptyl 4'-(4''-*n*-alkoxyphenylpropioloyloxy)biphenyl-4-carboxylates (1M7nOPPBCs).

n	liq to liq	Iso to TGB <sub>A</sub> *	TGB <sub>A</sub> * to C*
<i>(R)</i> and <i>(S)</i> Enantiomers		e.c. $\approx 0.99$ for both isomers	
13	95.4	94.1	88.3
$\Delta H$	0.6	0.5	0.06
15	96.3	91.6	90.6
$\Delta H$	0.9	0.2	0.08
14	95.7	93.8	89.7
$\Delta H$	0.9	0.3	0.04
<b>Racemate</b>			
14		97.7	90.3
$\Delta H$		1.24	0.05

The presence of a liquid to liquid transition in these systems is one of the more intriguing aspects of the affects that chirality has in ordered fluid systems. Just why this transition should occur, and what is the nature/structure of the liquid phase which is present between the TGB phase and the isotropic liquid, are questions that have yet to be resolved. However, it is possible that the intermediate liquid phase is similar in nature to the Blue Fog phase<sup>3</sup> (or Blue Phase III) which is found to occur between Blue Phase II and the isotropic liquid. It is possible to speculate that the intermediary liquid phase has short range ordering of the molecules, and that when the TGB phase melts either the lattice of defects melts first leaving clusters of smectic A cybotactic-like groups surrounded by a normal liquid, or the smectic A regions of the TGB phase melt first leaving a network of screw dislocations floating in an amorphous liquid. This type of phase could be called an entangled flux phase.<sup>33</sup>

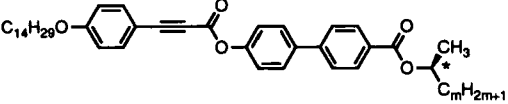
#### 2.4. Increasing the Peripheral Terminal Chain at the Chiral Centre

In the introduction section of this article trapping or restricting the motion of the chiral centre was discussed in terms of its increased effect on the molecular chirality of the system. For example, by increasing the length of a terminal aliphatic chain appended to the chiral centre it is expected that it will become buried in the overall structure of the molecule, thereby effectively damping the rotational freedom. This hypothesis was tested on the series of materials that exhibited TGB phases, thus the (*R*)- and (*S*)-1-methylalkyl 4'-(4''-*n*-alkoxyphenylpropioloyloxy)biphenyl-4-carboxylates (1MmnOPPBCs) were prepared.<sup>34</sup> The results obtained for the transition temperatures of some of the C<sub>14</sub> homologues are listed in Table V. It is interesting to note that the temperature range of the TGB<sub>A</sub> phase falls as the terminal aliphatic



TABLE V

Transition temperatures (°C) for 1-methylalkyl 4'-(4''-*n*-tetradecyloxyphenylpropioxyloxy)biphenyl-4-carboxylates



m	Iso to Iso	Iso to A* or TGB <sub>A</sub> *	A* or TGB <sub>A</sub> * to C*	C* to C* <sub>ferri</sub>	C* <sub>ferri</sub> to C* <sub>anti</sub>	Recryst
6	95.7	93.8	89.7	[53.4]	[42.5]	37.2
8	96.5	91.0	89.6	[38.6]		52.0
10	94.5	89.8	89.3			67.4

Where [ ] denotes a monotropic transition.

chain is increased in length, whereas the temperature ranges of the intermediary liquid phase increase and then decrease. This second observation is possibly more to do with the stability of the underlying TGB phase because upper transition temperatures for the intermediary liquid phase do not vary greatly. In an analogous way the ferri- and anti-ferroelectric phases appear to be suppressed with increasing peripheral chain length, but this issue is not as clear cut as that for the clearing point trends because the melting/recrystallization temperatures rise sharply with increasing chain length.

This study suggests that the effect of chirality diminishes with increasing terminal chain length. This may well be true for these materials, as increasing the length of the peripheral chain to greater than six carbon atoms may not have much affect on the rotational disposition of the chiral centre. In fact, the reverse might be the case and that by increasing the chain length we may be diluting the effects of chirality simply by increasing the relative size (volume) of the molecular structure.

For the series (*R*)- and (*S*)-1-methylalkyl 4'-(4''-*n*-alkoxyphenylpropioyl-oxy)biphenyl-4-carboxylates (1MmnOPPBCs) where the peripheral alkyl chain is eight or ten carbon atoms in length and the alkoxy chain is varied, similar results are obtained as for the 1-methylheptyl homologues discussed earlier except for the fact that TGB, ferrielectric, and antiferroelectric phases are not so prevalent; the properties of these two series are therefore not discussed in detail here. However, it is interesting to note that the intermediary liquid phase is found to occur even in homologues where there is no TGB phase present, as shown by the DSC data given in Figure 21 for the (*R*) and (*S*)-1-methylnonyl 4'-(4''-*n*-alkoxyphenylpropioyl-oxy)biphenyl-4-carboxylates (1M9nOPPBCs). If the clearing point enthalpies of this series are plotted as a function of increasing chain length, then again we see the values fall sharply. However, if the sum of the liquid to liquid crystal and liquid to liquid transitions is determined then it can be seen that the overall enthalpies associated with the clearing point process rise (see Figure 22), but much of the activity is taking place in the liquid phase and not at the liquid to liquid crystal transition.

Changing the length of the lateral group at the chiral centre from methyl to

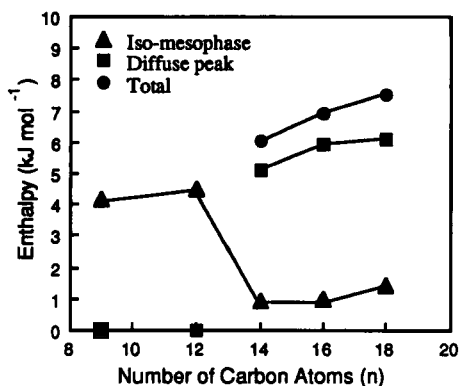


FIGURE 21 Enthalpies ( $\text{kJ mol}^{-1}$ ) for transitions occurring at or near the clearing point for the (*R*)- and (*S*)-1-methylnonyl 4'-(4''-*n*-alkoxyphenylpropionyloxy)biphenyl-4-carboxylates (1M9nOPPBCs). The total enthalpy value for the liquid-liquid and liquid-liquid crystal transitions is also shown.

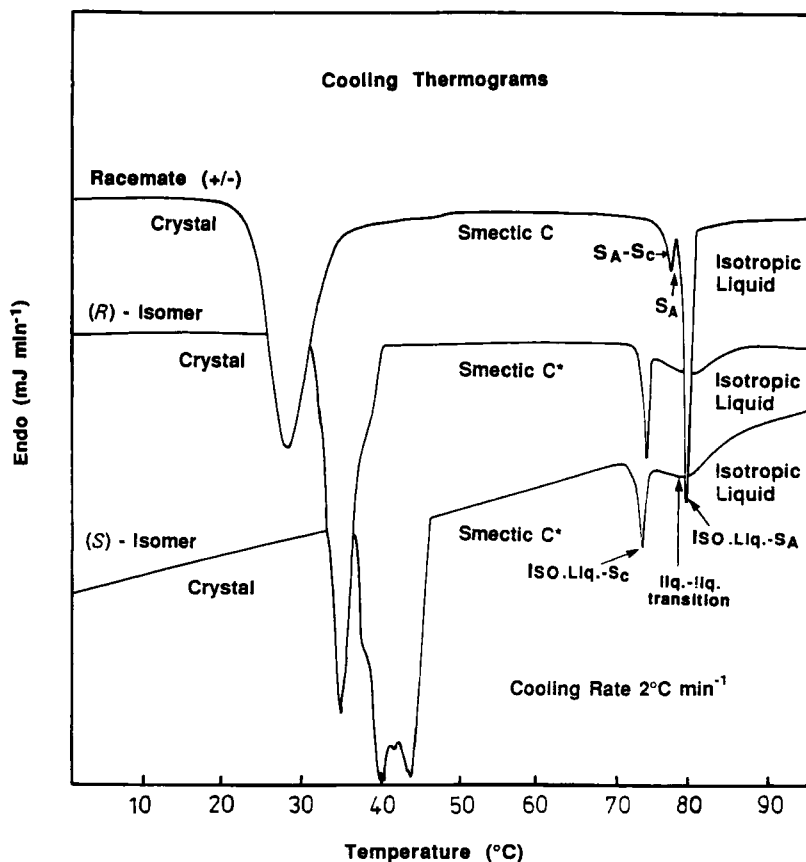


FIGURE 22 The DSC cooling thermograms for the (*R*), (*S*) and racemic forms of 1-methylheptyl 4'-(3''-fluoro-4''-*n*-tetradecyloxyphenylpropionyloxy)biphenyl-4-carboxylate.

propyl for instance has the effect of suppressing all liquid crystal transitions, and in the case of the C<sub>14</sub> ethyl branched homologue no liquid crystal phases are observed. This study indicates that by increasing the size of the lateral substituent in order to restrict the rotational freedom, we have essentially increased the lateral steric repulsive interactions to such an extent that the molecules cannot pack easily together to form a mesophase.

## 2.5. Lateral Substitution in the Core of the Mesogen

In the previous sections we have been primarily concerned with the effects of changing the terminal alkoxy chain length and the peripheral chain lengths of the aliphatic moieties attached to the chiral centre, in this part we examine the effect on TGB phases of the introduction of substituents into the aromatic core of the mesogen. In particular, the effects of the introduction of lateral fluorine atoms into the phenylpropiolate portion of the molecule are highlighted. Table VI shows the comparison between the transition temperatures of fluorinated and unfluorinated systems. The unfluorinated materials have slightly higher temperatures than their analogous fluorinated compounds. With a fluorine atom pointing in towards the centre of the core (in the 2 position) TGB phases appear to be more stabilized or at least of approximately the same temperature range as the TGB phases found for the unfluorinated analogues. However, these materials also appear to exhibit TGB<sub>A</sub>\* to smectic A\* transitions unlike the hydrogenous forms.

The 3-fluoro systems are the more remarkable members of this series of com-

TABLE VI

Transition temperatures (°C) for the (*R*)- and (*S*)-1-methylheptyl 4'-(3''-fluoro-or 2''-fluoro-4''-*n*-alkoxyphenylpropioloyloxy)biphenyl-4-carboxylates (1M7nOPFPBCs)

n	X,Y	Iso to A* or TGB <sub>A</sub> *	TGB <sub>A</sub> * to A*	Iso to C*	A* or TGB <sub>A</sub> * to C*	C* to C* <sub>ferri</sub>	C* <sub>ferri</sub> to C* <sub>anti</sub>	Recryst
14	H,H	93.8			89.7	[53.4]	[42.5]	37.2
14(+/-)	H,H	97.7†			90.3†			
14(R)	F,H			75.4				49.6
14(S)	F,H			75.5				62.7
14(+/-)	F,H	81.5†			79.3†			44.8†
14(R)	H,F	85.8	80.8		72.6			37.8
14(S)	H,F	87.0	82.9		73.5			39.2
14(+/-)	H,F	87.6†			76.8†			33.6†

Where [ ] denotes a monotropic transition,

† denotes a phase transitions for an achiral material; for these transitions the asterisk should be omitted from the column heading,

(+/-) denotes the racemic form.

pounds. It can be seen that the optically active variants do not exhibit TGB phases, but instead possess a direct isotropic to smectic C\* transition. However, the racemate displays somewhat different behaviour in that a smectic A phase is inserted between the isotropic liquid and the smectic C phase. The phase transitions also occur at higher temperatures in the racemic modification in comparison to the enantiomers. This indicates that the nature of the chirality has the effect of suppressing phase transitions, and in particular the isotropic to smectic A\* transition to a point where it occurs below that of the transition to the C\* phase in the enantiomers (if it were permitted). For the enantiomers, a DSC scan shows that a liquid to liquid transition appears at the same temperature where the A to C transition occurs for the racemate, as shown in Figure 22.

This is quite a remarkable effect as the clearing point temperature is suppressed by almost 4°C by the introduction of chirality into the system, and this suppression is enough to negate the formation of a smectic A\* phase in the enantiomers. The broad peak seen in the DSC trace for the liquid to liquid transition once again suggests that the intermediary liquid phase has short range order possibly of a cybotactic nature.

It is also interesting to note that fluoro-substitution adversely affects the presence of ferroelectric and antiferroelectric phases. The ferro- to ferri- and ferri- to antiferroelectric transition temperatures were found to be reduced by at least 15°C in some cases.

Miscibility studies of the (*R*)-3-fluoro-isomer with the (*S*)-3-fluoro-enantiomer show the generation, and stabilization, of a smectic A phase through the formation of a TGB<sub>A</sub> phase, and possibly a TGB<sub>C</sub> phase. Further details of this unusual behaviour are published elsewhere.

## 2.6. Terminal Linking Groups, Esters versus Ketones

The (*S*)-4-(2-methyloctanoyl)biphenyl 4-*n*-alkoxyphenylpropiolates (1M7COBnOPs), shown in Figure 23, were also prepared and the results obtained on their liquid-crystalline and physical properties were compared with those for the analogous series (*R*)- and (*S*)-1-methylheptyl 4'-(4''-*n*-alkoxyphenylpropioloyloxy)biphenyl-4-carboxylates (1M7nOPPBCs).<sup>34</sup>

The homologous series was selected for synthesis because it possesses a strongly polar “carbonyl” moiety, that is located adjacent to the chiral centre. The dipole associated with the carbonyl functional group is considered to be stronger than that for an ester group, therefore, this study was expected to produce information on the effect that the stronger lateral dipole of the molecules has on the formation of TGB and antiferroelectric phases.

The transition temperatures of the (*S*)-4-(2-methyloctanoyl)biphenyl 4-*n*-al-

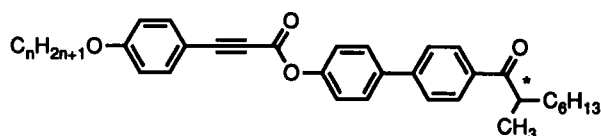


FIGURE 23

kyloxyphenylpropiolates (1M7COBnOPs) determined by a combination of thermal optical polarized light microscopy and differential scanning calorimetry are shown in Table VII, and depicted graphically in Figure 24.

It can be seen from the graph, shown in Figure 25, that the clearing point transition temperatures are almost independent of *n*-alkyl chain length (*n*) over the number of homologues studied. The transition temperatures are almost constant at a value of approximately 107°C. This form of behaviour is clearly different from that observed for the analogous ester series. In the case of the esters the clearing points fall with increasing the *n*-alkoxy chain length (*n*). Furthermore, the clearing points of the ketones are higher than those of the esters. These results indicate that the "liquid crystallinity" of the ketones is stronger than that in the analogous esters. Thus, it is possible that the stronger dipole associated with the carbonyl moiety and its adjacent position to the chiral centre may play an important role in stabilizing the mesophase formation. However, unlike the esters, the "ketone" homologous series was found not to exhibit TGB phases. This is because the increased isotropic liquid to smectic A\* and lower smectic A\* to smectic C\* transition temperatures for the ketones has the effect of stabilizing the smectic A\* phase over approximately a 20°C range, even for the longest chain length studied (*n* = 18). The wideness of the temperature range of the smectic A\* phase is undesirable for the emergence and stabilization of TGB phases, because the TGB phase requires fluctuations from neighbouring phases to be present.

These results can be augmented, and to some extent confirmed, by examination of the DSC thermograms of the ketones and comparing them to those of the esters, see Tables III and VII, and compare Figures 20 and 26. Unlike the esters, the

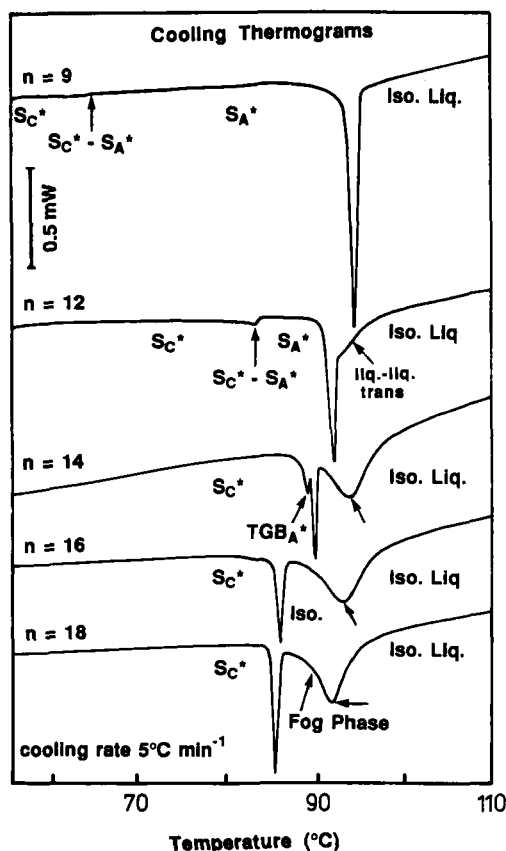
TABLE VII

Transition temperatures (°C) and enthalpies of transition (kJ mol<sup>-1</sup>) for the (*S*)-4-(2-methyloctanoyl)biphenyl-4-*n*-alkoxyphenylpropiolates (1M7COBnOPs)

<i>n</i>	Iso to A*	A* to C*	C* to S <sub>3</sub>	mp <sup>†</sup>	Recryst
9	107.5	[72.0]		73.0	36.8
ΔH	4.2	0.3		43.8	13.4
12	108.6	85.3	[33.4]	56.6	-2.2†
ΔH	5.2	0.3	3.3	38.6	8.6
14	106.7	89.0	[38.2]	66.0	-4.6†
ΔH	5.6	0.4	3.7	37.6	6.2
16	106.6	86.8	[42.5]	61.3	26.0
ΔH	6.2	0.2	4.9	42.0	9.3
18	107.7	91.2	[48.5]	58.5	30.6
ΔH	6.5	0.3	6.8	56.8	13.0

Where [ ] denotes a monotropic transition temperature,

† denotes a transition temperature determined by DSC.



enthalpy values for the clearing points were found to increase as the  $n$ -alkoxy chain length ( $n$ ) is lengthened. In the case of the analogous ester series, the first order isotropic liquid to smectic  $A^*$  transition has a strong tendency to become second order in nature as the series is ascended, however, for the ketones the reverse is the case. Calorimetric thermograms show a strong sharp peak corresponding to the isotropic liquid to smectic  $A^*$  transition for all of the members of the ketone series studied. Moreover, the thermograms show no large diffuse peak just above the clearing transition, which was found in the case of the esters.

From DSC measurements, the smectic  $C^*$  to smectic 3 transitions for the ketones also appear to be strongly first order, unlike those normally associated with the smectic  $C^*$  to antiferroelectric transition which tend to be second order. These observations support results obtained from optical microscopy which suggest that  $S_3$  is not an antiferroelectric phase, but has long range ordering of some form. The esters unlike the ketones were found to exhibit antiferroelectric and ferroelectric phases.

The smectic  $C^*$  and  $S_3$  phases and their accompanying phase transitions, were investigated by thermal polarized-light microscopy on a variety of differently aligned

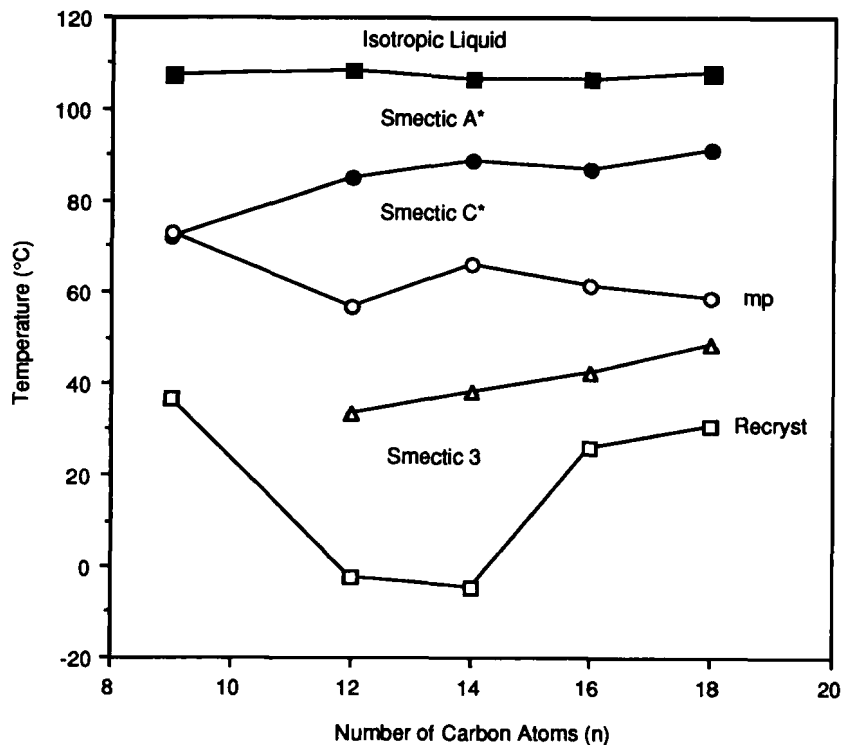


FIGURE 25 Transition temperatures ( $^{\circ}\text{C}$ ) shown as a function of increasing  $n$ -alkoxy chain length ( $n$ ) for the (*S*)-4-(2-methyloctanoyl)biphenyl 4- $n$ -alkoxyphenylpropiolates (1M7COBnOPs).

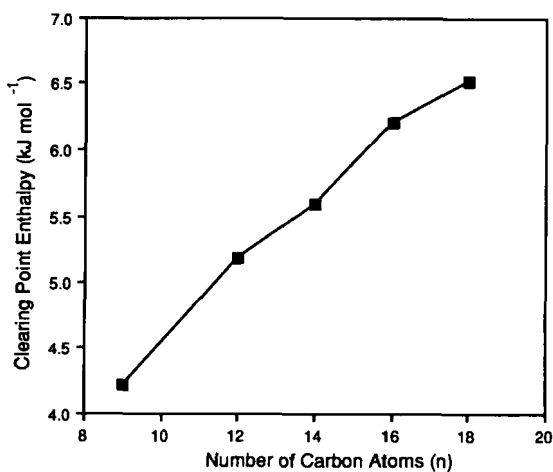


FIGURE 26 The clearing point enthalpies ( $\text{kJ mol}^{-1}$ ) plotted as a function of alkoxy chain length ( $n$ ) in the (*S*)-4-(2-methyloctanoyl)biphenyl 4- $n$ -alkoxyphenylpropiolates (1M7COBnOPs).

specimens of members of the "ketone" series. For example, homogeneous alignment was achieved by introducing each individual homologue into a polyimide-(PI)-coated and unidirectionally buffed cell (spacing  $3\text{ }\mu\text{m}$ ). At the transition from the smectic C\* to smectic 3 phase for the dodecyloxy homologue, a well-defined textural change was observed. This transformation was quickly followed by a second textural change, which was quite similar to that observed at the smectic C\* to antiferroelectric transition. After the second change of texture, the extinction direction in the sample was found to be along the layer normal which is consistent with the smectic 3 phase of the dodecyloxy homologue having antiferroelectric character. However, the hexadecyloxy and octadecyloxy members showed only a single textural change at the smectic C\* to smectic 3 transition, and unlike the dodecyloxy homologue these smectic 3 phases did not exhibit a texture that was characteristic of an antiferroelectric phase. In the case of the smectic 3 phase of the tetradecyloxy compound, an extremely small portion of the specimen possessed an antiferroelectric texture. Thus, these microscopic studies are somewhat inconclusive as to whether the smectic 3 phase of the ketone series, like the analogous esters, is antiferroelectric in nature or not. Switching studies were used to elucidate the situation further, and were found to confirm the presence of antiferroelectric properties for the S<sub>3</sub> phase. However, the differences in the textures and DSC data, with respect to the corresponding studies performed on the esters, suggests that although the S<sub>3</sub> phase may be ferroelectric it may not be of the same type as the antiferroelectric phase found in the phenylpropiolate esters and related homologous series. It is also interesting to note in this context that the "ketone" series does not appear to exhibit ferrielectric phases whereas the propiolate esters do, and that this may affect the textures and characters of the transitions.

In order to examine the effect that the increased dipolar character has on other chiral related properties, the spontaneous polarization was measured as a function of temperature for each of the members of the "ketone" series; the results obtained are as shown in Figure 27. The maximum value for the spontaneous polarization for each member was found to be relatively large, approaching  $200\text{ nC cm}^{-2}$  in some cases. It is interesting to note that the relative spontaneous polarization (i.e., measured at the same reduced temperature) falls as the alkoxy chain is lengthened. This could be due to the fact that as the series is ascended the molecular length increases, thereby reducing the dipole density and causing a dilution in the dipole concentration. Effectively, as the series is ascended the measured "polarity" (Ps) which is directly related to the "molecular chirality" of the materials decreases. However, the values obtained for the spontaneous polarization for the "ketone" series are larger than those measured for the analogous propiolate esters. For example, the value of the spontaneous polarization for the dodecyloxy member and analogous propiolate ester, measured at  $10^\circ\text{C}$  below the smectic A to smectic C\* transition ( $T_{AC} - T = 10^\circ\text{C}$ ), are compared in Figure 28. The larger polarization value for the dodecyloxy member of the ketone series is probably attributable to the larger dipole moment of the carbonyl group in relation to the ester group in the vicinity of the chiral centre.<sup>35</sup>

Thus, this comparative study shows how the lateral dipolar character associated with the "chirality" and the linking group of the system can affect the value of a



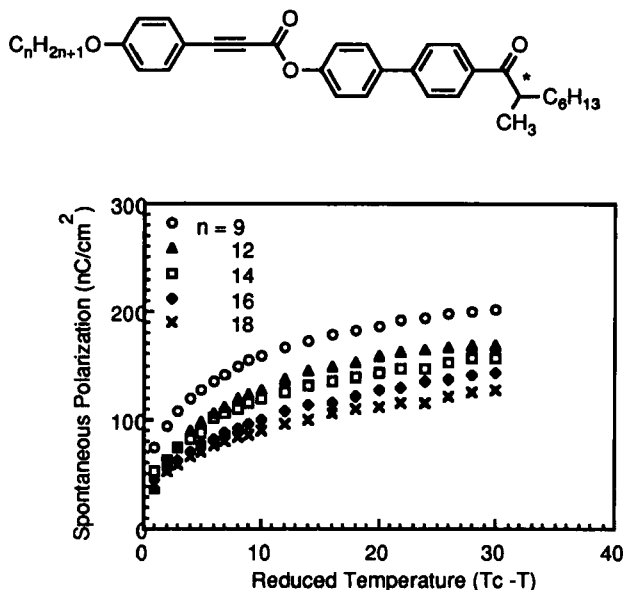


FIGURE 27 The spontaneous polarization (nC cm<sup>-2</sup>) measured as a function of the reduced temperature, (T<sub>AC</sub> - T) (°C), for members of the (S)-4-(2-methyloctanoyl)biphenyl 4-n-alkoxyphenyl-propiolates (1M7COBnOPs).

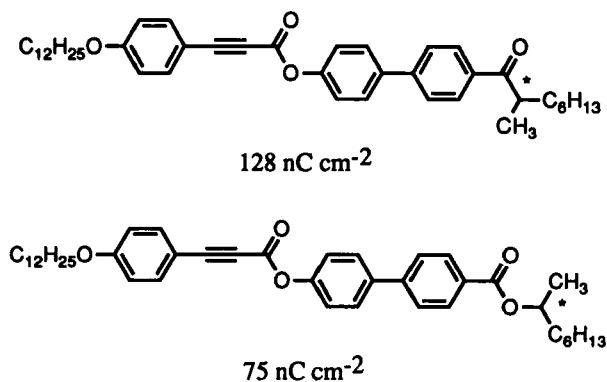


FIGURE 28 Comparison of polarization values measured at 10°C below the smectic A to smectic C\* transition for analogous ketone and ester homologues.

macroscopic property such as the polarization, but at the same time these changes do not necessarily affect other chirality dependent properties to the same degree, e.g., the incidence of TGB phases. In fact one possible conclusion that can be drawn from this study is that the incidence and stability of TGB and smectic A\* phases, is affected more by the steric structure of the materials under consideration than the spontaneous polarization is, on the other hand the spontaneous polarization is more affected by the dipolar nature of the material.

## 2.7. The Effect of Dipolar Groups at the Chiral Centre

A large number of studies have been performed on a variety of propiolate and benzoate biphenyl esters where a polar atom or group was positioned at the chiral centre. In more cases studied, that are related to the liquid crystal systems discussed previously in this article, cholesteric phases were introduced into the phase sequences. For example, in the propiolates discussed in section 2.3 no cholesteric phases were found to occur, and instead some members of the series exhibited direct isotropic liquid to TGB phase transitions. Replacement of the lateral methyl group by a more polar group at the chiral centre generally resulted in the introduction of a cholesteric phase, and consequently a TGB phase was found to mediate the transition to the smectic state.<sup>36</sup> However, in these homologous series for members that exhibit direct transitions from the liquid to the smectic state, no TGB phases were detected at the phase transition. As with other materials, it was found that short terminal peripheral chains on the external side of the chiral centre did not favour the formation of TGB phases, however, extension of this chain was found to lead to an increase in the chirality of the system, and thereby to a stabilization of TGB phases.

The structures of the first pair of homologous series that we can compare are shown in Figure 29; their transition temperatures are given in Tables VIII and IX, and shown as a function of alkoxy chain length in Figures 30 and 31, respectively.

These materials have in common the 2-chloropropyl chiral end group, which is attached to the core of the system via an ester linkage. In both series no TGB phases are observed, but wide temperature range smectic A\* phases are found. This might explain the lack of TGB phases because, due to the wide temperature ranges, the stable A\* phase will not experience strong fluctuations from adjacent phases. Moreover, the size of the alkyl chain attached to the peripheral side of the chiral centre is relatively small in size (a methyl group), and therefore the rotation of the chiral centre with respect to the core structure is likely to be quite free. This freedom would in effect "smear out" the dipole associated with the optically active centre (as the chiral centre rotates rapidly about the C1—C2 bond), and thereby reduce the effective "chirality" of the system.<sup>37</sup> Thus, it might be expected that the smearing out of the lateral dipolar coupling would have an effect on the mag-

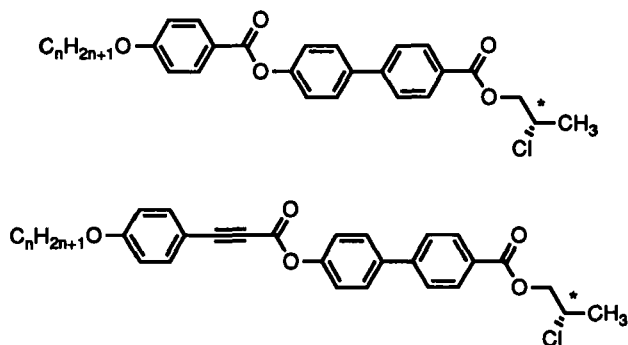
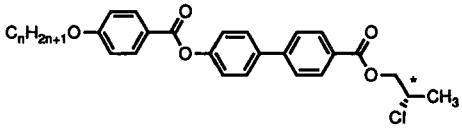


FIGURE 29

TABLE VIII

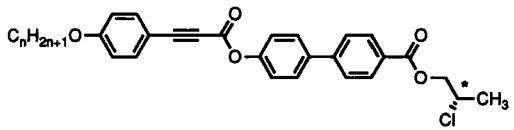
Transition temperatures (°C) for the (*S*)-2-chloropropyl  
4'-(4''-*n*-alkoxybenzoyloxy)biphenyl-4-carboxylates



n	Iso to Ch	Iso to S <sub>A</sub> *	Ch to S <sub>A</sub> *	S <sub>A</sub> * to S <sub>C</sub> *	mp	Recryst
7	194.5		186.4	79.0	102.2	65.5
8	193.0		190.1	72.7	94.6	55.7
9		191.6		67.7	90.2	65.5
10		191.6		58.4	82.9	43.6
11		190.3		49.7	82.3	55.2
12		188.3			76.1	53.6
13		186.4			70.2	48.5
14		185.4			85.5	55.1

TABLE IX

Transition temperatures (°C) for the (*S*)-2-chloropropyl  
4'-(4''-*n*-alkoxyphenylpropiolyloxy)biphenyl-4-carboxylates



n	Iso to Ch	Iso to S <sub>A</sub> *	Ch to S <sub>A</sub> *	mp	Recryst
9	166.0		137.0	102.6	62.0
12	157.4		149.0	76.9	65.1
14	150.1		149.2	69.9	44.4*
16		150.8		87.7	41.8
18		149.5		91.6	47.5

nitude of the spontaneous polarization in smectic C\* phases. Similarly, this rotational freedom might also be expected to effect the steric interactions to some degree, and hence the pitch in helical phases such as the cholesteric and smectic C\* phases (see later).

Contrasting the benzoates with the propiolates reveals some interesting comparisons; for instance, the propiolates have much lower transition temperatures overall, which is unusual considering that they have larger structures with more extensively delocalised regions. The benzoates also exhibit ferroelectric smectic C\* phases, whereas the propiolates do not. In both series Blue Phases are not found to mediate the cholesteric to isotropic liquid transition, moreover, the pitch of the helical macrostructure in the cholesteric phase appears to be in the micrometer

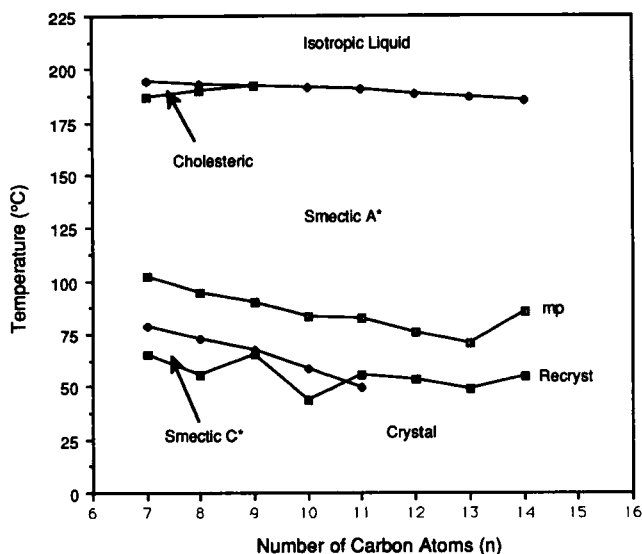


FIGURE 30 Transition temperatures (°C) shown as a function of  $n$ -alkoxy chain length ( $n$ ) for the (S)-2-chloropropyl 4'-(4''- $n$ -alkoxybenzoyloxy)biphenyl-4-carboxylates.

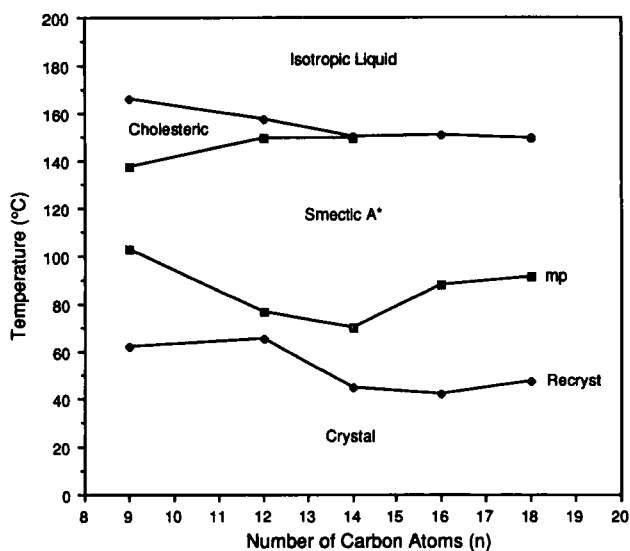


FIGURE 31 Transition temperature (°C) shown as a function of  $n$ -alkoxy chain length ( $n$ ) for the (S)-2-chloropropyl 4'-(4''- $n$ -alkoxyphenylpropioloyloxy)biphenyl-4-carboxylates.

range indicating that the twisting power in these materials is not particularly strong. These observations support the view given earlier that the shortness of the peripheral chain appended to the chiral centre is responsible for the weaker chiral properties of these two homologous series.

Systems such as the ones described above were investigated further through the extension of the peripheral chain on the external side of the chiral centre. It was

expected, for reasons given earlier, that by extending this chain the rotational freedom of the chiral centre would be reduced through a reduction in the freedom to conformationally change the molecular structure (i.e., through a restriction of the bond rotation near, or about, the chiral centre itself) and through rotational hindrance about the molecular long axis as a whole. Therefore, in the next section we present results on two such homologous series, see Figure 32. These series are selected as examples of the many closely related series that have been synthesised, however, the results described are consistent, and somewhat typical of the other series that are not reported here.

The two series, the (*S*)-2-chloro-4-methylphenyl 4'-(4''-*n*-alkoxybenzoyloxy)biphenyl-4-carboxylates and the (*S*)-2-chloro-4-methylpentyl 4'-(4''-*n*-alkoxyphenylpropionyloxy)biphenyl-4-carboxylates, were selected for synthesis because the chiral group can be readily prepared from (*S*)-leucine. This group allows us to extend the terminal chain on the external side of the chiral centre, however, it does have the slight problem of also introducing a branching point in the chain as well, albeit in the terminal position.

The transition temperatures of the benzoates and the propiolates are given in Tables X and XI, and depicted graphically in Figures 33 and 34. It can be seen from these results that the transition temperatures are much reduced for the derivatives of leucine over the derivatives of alanine (the 2-chloropropyl compounds). Moreover, the longer chain compounds exhibit well-defined Blue Phases at the transition from the isotropic liquid to the cholesteric phase, and Twist Grain Boundary phases at the transition from the cholesteric to the smectic A\* phase. However, no TGB phases are observed at the isotropic liquid to smectic A\* transition as they were found to occur in the propiolates described in section 2.3. The presence of both of these phases suggests that the "effects of chirality" are stronger in the 2-chloro-4-methyl derivatives than the 2-chloropropyl analogues,<sup>38</sup> however, they are not as strong as those operating for the 1-methylheptyl compounds. This is probably due to the fact that the chiral centre is removed from the core by one more atom in the case of the materials derived from amino acids, and hence it has more rotational freedom associated with it in comparison to the 1-methylheptyl moiety where the motion of the lateral methyl group is expected to be severely restricted by the adjacent ester function. It is also interesting to note that the TGB

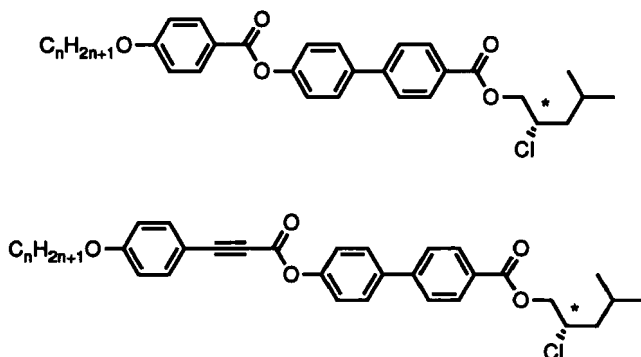
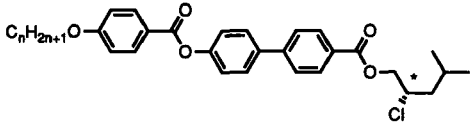


FIGURE 32

TABLE X

Transition temperatures (°C) for the (*S*)-2-chloro-4-methylpentyl  
4'-(4''-*n*-alkoxybenzoyloxy)biphenyl-4-carboxylates

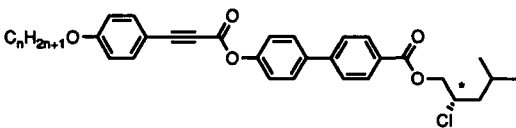


n	Iso to BP†	BP to Ch	Ch to TGB <sub>A</sub> *	TGB <sub>A</sub> * to A*	Iso to A*	A* to C*	mp	Recryst
7	156.1	153.2	144.9	144.2		119.2	73.4	40.9
8	155.4	148.3	146.8	146.0		115.1	75.0	53.7
9	150.4	145.5	145.4	144.6		121.0	74.9	41.8
10	149.7	146.8	145.6	144.8		121.9	64.4	34.0
11	148.1	146.8	145.8	145.0		124.2	69.4	57.5
12	145.6	145.0	144.8	144.1		122.0	68.8	49.8
13					142.5	121.7	73.5	50.2
14					142.0	121.4	76.7	53.0

Where † denotes a transition to Blue Phase III or Blue Phase II, the transitions between the various Blue Phases are not reported in detail here, but will be published elsewhere.

TABLE XI

Transition temperatures (°C) for the (*S*)-2-chloro-4-methylpentyl  
4'-(4''-*n*-alkoxyphenylpropioloyloxy)biphenyl-4-carboxylates



n	Iso to BP†	BP to Ch	Ch to TGB <sub>A</sub> *	TGB <sub>A</sub> * to A*	A* to C*	mp	Recryst
9	129.4	128.3	100.4	96.8	79.9	67.8	32.6
12	122.7	122.5	108.1	106.8	93.2	73.3	50.7
14	119.9	116.4	110.9	109.7	98.1	68.5	38.7
16	117.5	116.3	114.6	113.6	101.2	59.9	31.4
18	115.4	114.9	114.2	113.4	99.9	56.1	43.3

Where † denotes a transition to Blue Phase III or Blue Phase II, the transitions between the various Blue Phases are not reported in detail here, but will be published elsewhere.

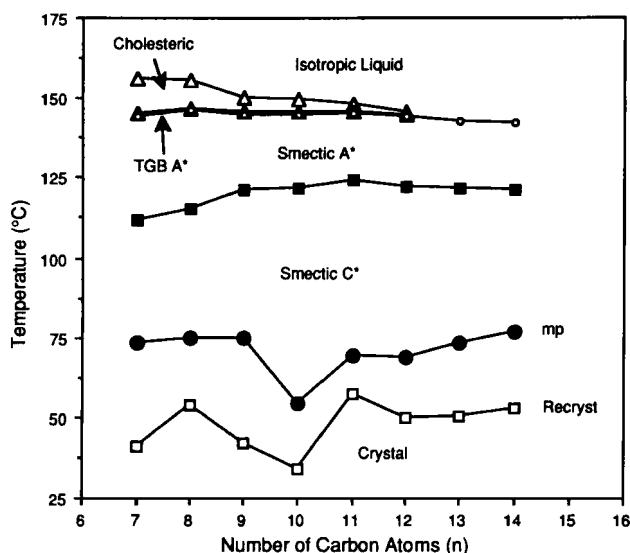


FIGURE 33 Transition temperatures (°C) for the (S)-2-chloro-4-methylpentyl 4'-(4''-n-alkoxybenzoyloxy)biphenyl-4-carboxylates plotted as a function of terminal alkoxy chain length.

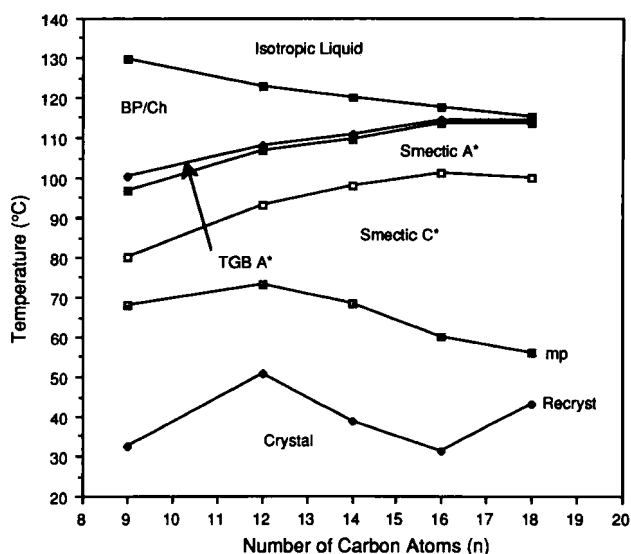


FIGURE 34 Transition temperatures (°C) for the (S)-2-chloro-4-methylpentyl 4'-(4''-n-alkoxyphenylpropioloyloxy)biphenyl-4-carboxylates plotted as a function of terminal alkoxy chain length.

phases seem to have longer temperature ranges in the benzoates in comparison to the propiolates, which is the reverse of the situation found for the 1-methylheptyl derivatives. Furthermore, it appears that the TGB phases are more stable at shorter alkoxy chain lengths in the benzoate derivatives of leucine than they are for the longer members. This latter effect may be due to the stabilization of the smectic A\* phase for the higher homologues.

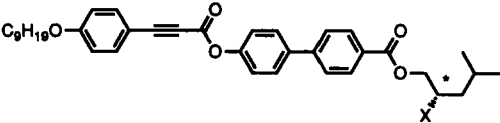
In both series derived from leucine, the smectic A\* temperature range is relatively long which might also account for the lack of TGB phases found at the transition from the isotropic liquid. The occurrence of TGB phases at the cholesteric to smectic A\* transition confirms Renn and Lubensky's model<sup>4</sup> for the TGB phase, and these compounds serve as the first examples of low molar mass materials to exhibit this defect stabilized phase at the cholesteric to A\* transition. It is also interesting that these materials provide us with examples of two frustrated phenomena in the same system, i.e., Blue Phases, where the pressure to form twisted structures in three dimensions is alleviated by the formation of a three-dimensional lattice of defects, and TGB phases where the competition between the need to form a layered structure and at the same time form a helix in the plane of those self-same layers results in the formation of another different type of lattice of defects. Thus, it can be seen that the effects of "chirality" and its competition with the normal structural aspects of liquid crystals can lead to novel phases being stabilized.

As part of this study we also varied the nature, size and polarity of the lateral group attached to the chiral centre, i.e., the halogen atom was varied. Thus, for a given *n*-alkoxy chain length (9 carbon atoms) and a terminal chiral group derived from leucine, the lateral halogen atom at the chiral centre was changed from fluorine to chlorine to bromine. The results obtained for the liquid-crystalline transitions of these materials are given in Table XII, and compared in a bar graph in Figure 35.

The results appear to show that as the size of the halogen atom is increased the clearing points fall, which suggests that the lateral steric repulsion increases as the series is ascended. The fluoro and chloro homologues exhibit TGB phases at the transition from the cholesteric to the smectic A\* phase, but no TGB phases are found to occur for the bromo analogue which may be due to the fact that the Blue Phase is absent. Both the fluoro and chloro compounds also exhibit frustrated Blue Phases in addition to TGB phases. The TGB and Blue Phase temperature ranges

TABLE XII

Transition temperatures (°C) for the (*S*)-2-halogeno-4-methylpentyl 4'-(4''-*n*-nonyloxyphenylpropioloyloxy)biphenyl-4-carboxylates

									
X	Iso to BP†	Iso to Ch	BP to Ch	Ch to SA*	Ch to TGBA*	TGBA* to A*	A* to C*	mp	Recryst
F	142.0		141.0		113.4	111.3	94.4	68.4	54.5
Cl	129.4		128.3		100.4	96.8	79.9	67.8	32.6
Br		123.6		94.4			72.3	72.1	37.8

Where † denotes a transition to Blue Phase III or Blue Phase II, the transitions between the various Blue Phases are not reported in detail here, but will be published elsewhere.



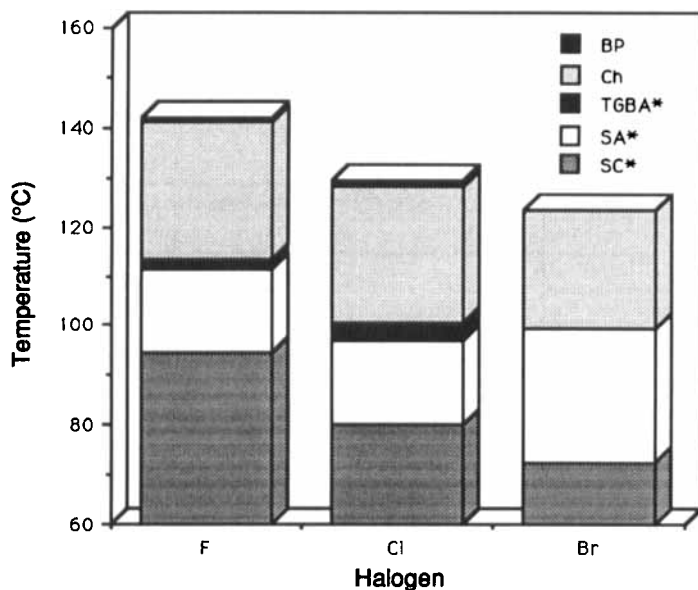


FIGURE 35 Comparison of the transition temperatures (°C) for the (*S*)-2-halogeno-4-methylpentyl 4'-*n*-nonyloxyphenylpropionyloxybiphenyl-4-carboxylates.

appear to be widest in the chloro homologue suggesting that the effects of chirality are felt strongest in this material. Certainly, both the dipolar and steric effects will be stronger in the chloro compound in comparison to the fluoro analogue, therefore we might expect stabilization of the frustrated phases. In the case of the bromo homologue, the bromine atom is so big that its rotational freedom is severely restricted, and hence the lateral repulsive interactions created by this will have adverse effects on the chiral interactions. Similarly, the loss of the cholesteric phase destabilises the formation of frustrated phases, therefore we cannot correctly evaluate the effect of chirality in this particular system. However, the increased pitch length of the helical macrostructure in the smectic C\* phase of this homologue, in relation to the other two, strongly suggests that the effects of chirality in the bromo compound are much weaker. Thus, this study provides an interesting, if somewhat inconclusive, study of the effects of the magnitude of the polarity and the size of the lateral substituent at the chiral centre on TGB and Blue Phase stabilities.

### 3. INVERSIONS IN CHIRAL PROPERTIES

In the previous sections the competition between chirality and phase structure was discussed in terms of the formation of Twist Grain Boundary phases. In this portion of the text we examine the effect of competition between chirality at the molecular and macroscopic levels. In particular the effect on the direction of the spontaneous polarization in ferroelectric phases and helical twist direction in cholesteric and smectic C\* phases will be discussed.

### 3.1. Inversions in Polarization Direction

At the 11th International Liquid Crystal Meeting at Berkeley<sup>39</sup> we described the first examples of ferroelectric materials, the (*S*)-2-methyl 4'-*n*-alkanoyloxybiphenyl-4-carboxylates (see Figure 36), where the spontaneous polarization inverts direction with respect to temperature in the ferroelectric C\* phase.<sup>40</sup> As each individual material (that exhibits this effect) was cooled from its Curie point the polarization was found first to increase, then level off and fall. The value was found to fall to zero at which point the polarization inverted direction and the value increased again. Throughout this process the helical pitch of the macrostructure of the smectic C\* phase was found to be relatively constant at a value of around 2–3  $\mu\text{m}$ , even through the inversion point for the polarization. Measurement of the unwinding voltage<sup>41</sup> was found to be very low except close to the crossover point where it increased in value to over 100 V  $\mu\text{m}^{-1}$ . Away from this point the helix is unwound by coupling to the polarization, however, in the region of the crossover the unwinding is due to coupling with the dielectric anisotropy of the material. Similarly the tilt angle follows much the same behaviour because it is dependent on the magnitude of the spontaneous polarization, thus at high temperatures in the ferroelectric phase the materials appear to switch in one particular direction relative to the polarity of the applied field, whereas at lower temperatures this direction is reversed.

These results can only be explained by a situation where the effective lateral dipole inverts with respect to temperature. There have been suggestions that the tilt angle in the smectic C\* mesophase approaches zero at the crossover because the apparent tilt angle determined by switching studies also becomes zero, but this can be discounted by the fact that the phase remains helical throughout this process and because the pitch does not vary much the tilt angle should also remain relatively constant. Therefore, the molecules are still tilted with respect to the layer planes at the crossover point, but the value of the polarization must be zero for the apparent tilt angle to be zero.

In this series of esters it is interesting to note that inversions do not occur for the heptanoyloxy and octanoyloxy homologues, but for all of the higher members of the series that were studied this effect was found to occur.<sup>42</sup> Moreover, the first two members of the series investigated have positive polarizations ( $\text{Ps}(+)$ ), whereas the others have negative polarizations ( $\text{Ps}(-)$ ) at high temperatures and positive values at low temperatures. The closely related materials shown in Figure 37 are unlike the 2-methylbutyl esters in that neither show inversions. In one case the chiral centre is located nearer (adjacent) to the core, whereas in the second example it is further removed from the core by an extra carbon atom. The 1-methyl analogues

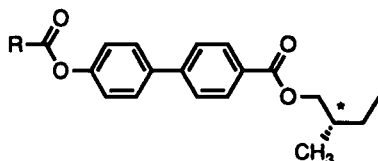


FIGURE 36

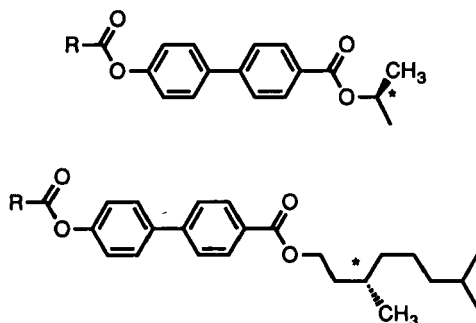


FIGURE 37

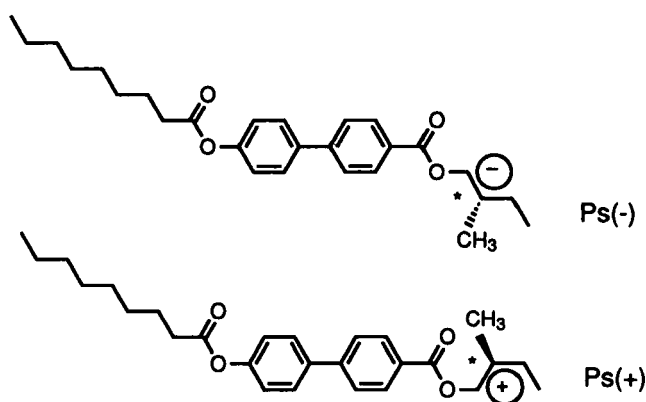


FIGURE 38

are found to have polarization directions that are in agreement with predictions derived from the Gray and McDonnell rules<sup>43</sup> relating spatial configuration to the location of the chiral centre relative to the core, whereas for the compounds derived from citronellol (the (*S*)-3-methyl-7-methyloctyl analogues) the reverse is the case. These results lead directly to the suggestion that in the 2-methylbutyl system there could be a competition between two or more chiral species that possess differing polarization directions, and that this competition leads to a change over in polarization properties.

One possibility is to ascribe the competition between various species to conformational changes in structure, examples of which are shown in Figure 38. In this concept two separate families of conformers would have differing polarization directions, and members of the two families would be able to interconvert via a small energy barrier. Therefore, at higher temperatures one species would dominate over the other, and at lower temperatures the reverse would be the case. Figure 38 shows a possible situation for two such conformers of the nonoyloxy compound. In the all trans conformer, the dipole located at the chiral centre will couple to the lateral dipole to give a resultant dipole pointing up out of the page (top figure), whereas in the gauche conformer the reverse will be the case and the orientation

of the chiral centre will cause the lateral dipole to be pointing down into the page (lower figure).

Assuming that these two species are interconvertible, then the spontaneous polarization will fall to zero when the two species compensate for each other. This process can in effect be modeled by assuming that the two species have separate polarizations associated with them, and that they interconvert via a small energy barrier ( $\Delta E$ ). The temperature dependence of the concentration of the two species can be assumed to affect the magnitude and direction of the polarization in the following way<sup>39,42</sup>;

$$P_s = [P_A e^{-\Delta E/kT} + P_B(1 - e^{-\Delta E/kT})](T_C - T)^\alpha$$

where  $P_A$  and  $P_B$  are the intrinsic polarizations of conformers A and B,  $\Delta E$  is the activation energy for the transformation from A to B,  $T_C$  is the A\* to C\* transition temperature and  $\alpha$  is an exponent which has a theoretical value of 0.5. The term  $(T_C - T)$  reflects the temperature dependence of the polarization, which is dependent to some degree on the tilt angle of the phase.

When used to model real data for the polarization in these materials, the value of  $\Delta E$  is found to be of the same magnitude as that for the rotation about the C2—C3 bond in *n*-butane. Furthermore, the values of the intrinsic spontaneous polarizations are roughly in agreement with theoretical values expected for conformer structures in the solid state (i.e. frozen-in structures). This model is, therefore, an attractive one, and it provides a simple rationale for such behaviour and the values determined for certain physical processes are not too different than those which might be expected.

### 3.2. Twist Inversions in Cholesteric Phases

In this section we extend the discussion of inversion phenomenon to the reversal of the helical structure in the cholesteric phase of the compound, (*S*)-2-chloropropyl 4'-(4''-*n*-nonyloxyphenylpropioloyloxy)biphenyl-4-carboxylate (9O2Cl3T). It was found that, on cooling from the isotropic liquid, a cholesteric phase was formed and then it underwent a twist inversion through an infinite pitch cholesteric phase ( $N_z^*$ ) on changing the temperature. Thus, at the inversion point a non-helical chiral nematic phase is formed. The structure of this material is shown below in Figure 39; the (*S*)-2-chloropropyl chiral end group is derived from (*S*)-alanine.

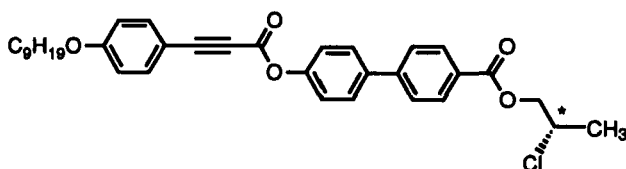


FIGURE 39

Thermal optical polarized light microscopy showed that this compound has the following phase sequence and transition temperatures (°C)

mp 102.6    Iso 166.0 Ch 142 N<sub>x</sub>\* 141 Ch 137.0 S<sub>A</sub>\* 62.0°C K

where mp is the melting point, Iso is the isotropic liquid and K is crystal phase.

Cooling this material between untreated glass slides gives a cholesteric phase which forms from the isotropic liquid in a typical fingerprint texture. The pitch of the cholesteric phase is found to increase as the temperature was reduced, and at about 150°C regions of pseudo-homeotropic texture become apparent as the cholesteric phase splits up into fingers which then gradually reduce in size. Further cooling results in the reformation of the cholesteric phase at approximately 141°C, however, this cholesteric phase has the opposite twist sense to the higher temperature cholesteric phase. The formation of the lower temperature cholesteric phase is promptly followed by a normal transition to a smectic A\* phase at 137°C.

Contact studies with the standard material (*S*)-4-*n*-decyloxybiphenyl 4'-(2-methylbutyl)benzoate<sup>44</sup> (Sed, note this compound is classified as a dextro material and not laevo as we reported previously)<sup>45</sup> were used to conclusively establish that the two cholesteric phases observed did indeed have opposite twist senses. Above the inversion point the cholesteric phase of the standard material and the propiolate had the same twist senses classifying the upper temperature cholesteric phase as *d* (left-hand helix). Below the inversion point the contact preparation exhibited a nematic discontinuity between the cholesteric phase of the standard and the test material indicating that they have opposite twists, thus proving that the lower temperature cholesteric phase has a right-hand helix (*l*).

Thermal analysis for (*S*)-2-chloropropyl 4'-(4''-*n*-nonyloxyphenyl)propiol-oyloxybiphenyl-4-carboxylate (9O2Cl3T) shows at the clearing point a single peak corresponding to the cholesteric to isotropic liquid transition. No evidence is found to suggest there are Blue Phases present. At 137°C the smectic A\* to cholesteric transition is clearly seen, but at the point where the helix inverts no associated enthalpy of transition is observed.

The pitch of the cholesteric phase of the material was measured by determining the distance between the dechiralization lines in the fingerprint texture of the mesophase. The value of the pitch as a function of temperature is shown in Figure 40, and the reciprocal value as a function of temperature is shown in Figure 41 (slight variations in the collected data were found and attributed to thermal decomposition of the material and surface pinning). From the first of these two figures, it can be seen that the pitch diverges in the temperature range of 140 to 145°C. The reciprocal plot shows that this value is approximately 141-2°C, which is in agreement with textural observations of the mesophase.

Although this is not the only material reported that exhibits this unusual phenomenon of a twist inversion in the cholesteric phase, it is possibly the first to show this behaviour when the molecule itself contains a single chiral atom in its structure. Typically other materials that show inversions tend to be diastereoisomeric, and hence twist inversions in their cases may be due simply to competition from the different chiral centres. In the case of a molecule that possesses a single

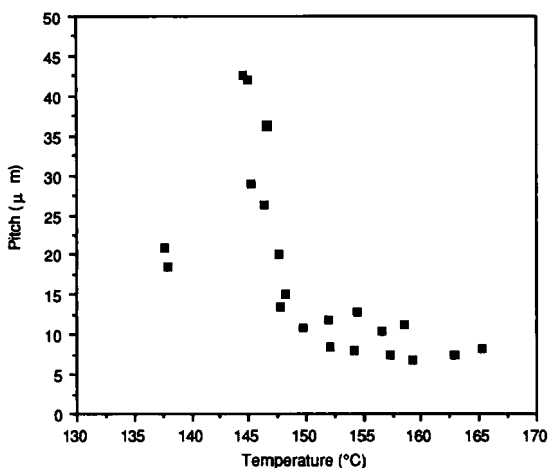


FIGURE 40 The variation in pitch length ( $\mu\text{m}$ ) of the helix as a function of temperature ( $^{\circ}\text{C}$ ) for the cholesteric phase of (*S*)-2-chloropropyl 4'-(4''-*n*-nonyloxyphenylpropioyloxy)biphenyl-4-carboxylate (9O2Cl3T).

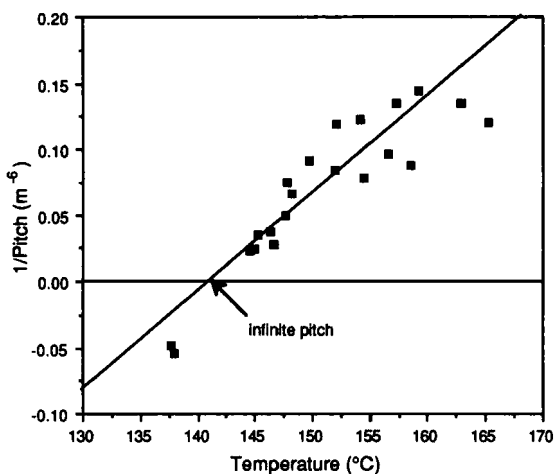


FIGURE 41 Reciprocal value of the pitch ( $\mu\text{m}^{-1}$ ) of the helix plotted as a function of temperature ( $^{\circ}\text{C}$ ) for the cholesteric phase of (*S*)-2-chloropropyl 4'-(4''-*n*-nonyloxyphenylpropioyloxy)biphenyl-4-carboxylate (9O2Cl3T).

chiral centre a different approach must be taken. As with the situation for materials that exhibit an inversion of the polarization, we could assume that the time averaged picture of the cholesteric phase may be one where there are a number of preferred stable rotational species, however, as the molecules are in dynamic motion the species will be interconvertable via a relatively small energy barrier. Consequently, the concentrations, and hence the number of densities, of the various species will be temperature dependent. As before we can now consider a situation where two competing classes of species exist which have opposite helical twist senses and “twisting powers.” As the temperature of the sample is altered the relative pop-

ulations of each species will change, and in the process the helical driving forces of the two classes may be internally compensated for by one another. At the compensation point the pitch of the mesophase diverges, and the helix will change sign.

Thus, as with the biphenylcarboxylates described in the previous section, in the case of the phenylpropiolates, we can define three staggered conformational structures produced by rotations about the C1—C2 bond (labeled A, B and C in Figure 42) for which there will be differing dipole directions and different steric structures.

It can be seen for conformer C that the chloro and methyl substituents, which have similar sizes, are positioned on equivalent, but opposite sides, of the long axis. Thus, it might be expected that the steric effects of these two off-axis substituents will compensate for one another. However, this is not the case for the other two conformers, A and B, where either one of the two substituents is located on (or along) the long axis of the molecule. Based on steric effects, it is quite possible, therefore, for the extreme conformers A and B to have opposing helical twist senses. For example, if the Newman projections of the two species are compared it can be seen that in conformer A where the terminal methyl group is positioned along the long axis of the molecule, chlorine points off to the right-hand side, whereas for the reversed situation, conformer B, with chlorine in the long axis the methyl group now points on the opposite, left-hand side of the long axis of conformer A. If the helix direction is sterically driven then its twist sense will be dependent on the packing and concentrations of the relative conformers in the pure material. Consequently, we expect that the twist senses of conformers A and B will oppose each other causing a twist inversion, but that the point at which the pitch of the cholesteric helix diverges need not necessarily occur at a 50:50 concentration of the two species A and B, as the two conformers will have different "twisting powers."

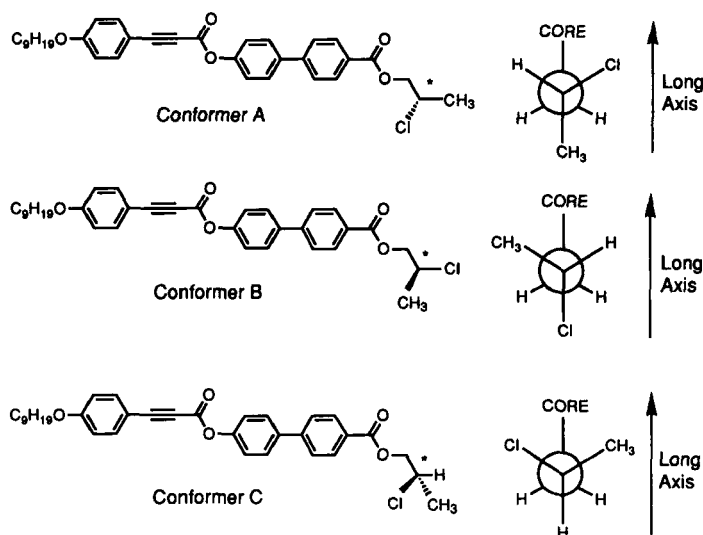


FIGURE 42 Conformational structures produced by rotations about the C1—C2 bond in (*S*)-2-chloropropyl 4'-(4''-*n*-nonyloxyphenyl-propioloyloxy)biphenyl-4-carboxylate (9O2Cl3T).

In principle these arguments should be extended to a whole range of conformers; i.e., even for rotations about bonds adjacent to the C1—C2 bond. Therefore, for each relative minimum energy position produced by rotation about the C1—C2 bond, the minimum energy positions for rotations about the C1—O bond should be superimposed in order to give a fuller picture of the global minimum energy positions of the various conformers. For example, Figure 43 shows three possible minimum energy conformers for a given rotation about the C1—O bond. Each conformer illustrated in this figure will have the opposite dipole and steric orientation relative to its corresponding all trans isomer shown in the previous Figure 42. Thus, a competition between conformers exists for the secondary structures in way similar to that obtained for the primary all trans conformers. However, it should be noted that these secondary structures will have substantially higher energies because of the increased steric hindrance.

In principle we have a similar situation for helix inversions as we do to polarization crossovers, therefore we might be tempted into believing that we could model this phenomena with an equation similar to that used to describe polarization inversions in the ferroelectric smectic C\* phase. However, the situation for the divergence of the pitch appears to be much more complex, and so far we have not been particularly successful in modeling this behaviour.

### 3.3. Twist Inversions in the Smectic C\* Phase

As with the cholesteric phase, inversions in the twist sense can also occur in the smectic C\* phase. The compound described above, which exhibits a twist inversion in the cholesteric phase, belongs to a homologous series where the smectic C\* phase is absent, however, when the terminal chain on the external side of the chiral centre is extended, smectic C\* phases become prevalent. Many of these materials appear to exhibit inversions in the helical twist sense as a function of temperature, however, the microscopic textures of the smectic C\* crossover are not as well-defined as those seen at the inversion point for the cholesteric phase. The compound that best exhibits this phenomenon is (*S*)-2-chloro-4'-methylpentyl 4'-*n*-hexadecyl-

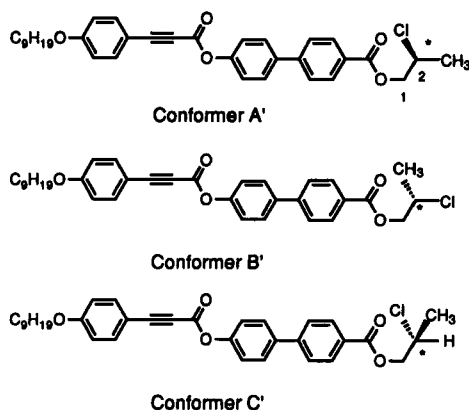


FIGURE 43 Secondary conformational structures for rotations about the C1—O bond in (*S*)-2-chloropropyl 4'--(4''-*n*-nonyloxyphenylpropionyloxy)biphenyl-4-carboxylate (9O2Cl3T).



oxyphenylpropioloyloxybiphenyl-4-carboxylate, the structure for which is shown in Figure 44.

This propiolate ester has the following transition temperatures:

Iso Liq 117.5 BPIII 116.8 BPI 116.3 Ch

Ch 114.6 TGB<sub>A</sub>• 113.6<sub>A</sub>• 101.2 S<sub>C</sub>• 31.4 Recryst mp 59.9°C

where the smectic C\* helix inverts between 49–43°C. At temperatures above the inversion point the helix is left-handed, and obviously below the crossover it is right-handed. Other members of this series also appear to exhibit twist inversions, however, the processes are usually accompanied by recrystallization which tends to obscure the effect.

For the hexadecyloxy compound, however, the helix is clearly seen to unwind and wind up again when a free-standing specimen of the material is viewed in the microscope. For example, when a freely suspended film is observed perpendicular to its surface then the viewing direction is parallel to the helical axis. Rotation of the upper polarizer can then be used to define the twist direction of the phase. Cooling results in the pseudo-homeotropic texture becoming birefringent to give a *schlieren* texture, further cooling gives a return to a pseudo-homeotropic texture that can be shown to have the opposite twist sense by rotating the upper polarizer of the microscope. Similarly, the smectic C\* phase can be shown to have a twist inversion by contact studies with (*S*)-2-chlorooctyl 4'-*n*-nonyloxyphenylpropioloyloxybiphenyl-4-carboxylate, which possesses a left-handed helix in its smectic C\* phase.<sup>46</sup> At higher temperatures in the smectic C\* phase the contact region shows no discontinuities, but as the temperature is lowered below the crossover point a discontinuity becomes apparent, with the two materials producing a region of infinite pitch length. These studies are still ongoing, but we suspect that the inversion is caused by a similar competition between conformers to those described earlier.

### 3.4. Inversions in Both Polarization and Helical Directions

So far we have described the results of materials where only one inversion occurs, and in the examples involving the smectic C\* phase we have produced materials where the polarization inverts and the helix does not and vice versa. In this section we will discuss the properties of a family of materials that show inversions in the helix in the cholesteric phase, in the helix of the smectic C\* phase, and in the direction of the spontaneous polarization.<sup>47</sup> Additionally, these materials exhibit

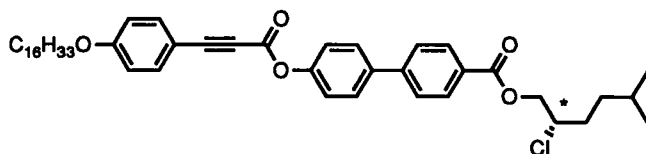


FIGURE 44

Blue Phases and TGB phases. Thus, we will discuss the properties of a series of 4-((2*S*,3*S*)-3-propyloxiranemethoxy)-2'-fluoro-4''-alkoxymethyl-[1,1':4',1'']-terphenyls which have structures based on the chiral (2*S*,3*S*)-oxiranemethanol moiety,<sup>48</sup> see Figure 45.

The first two compounds ( $C_3$  and  $C_5$  homologues) exhibit an inversion of helical twist sense in the cholesteric phase, separated by a region of infinite pitch. An additional inversion in the helical twist direction of the smectic  $C^*$  phase was observed in the case of the propyl member, and Twist Grain Boundary phases were also found in the second and third materials. The transition temperatures for the three compounds are given in Table XIII, and the physical properties for the first compound are highlighted in the following discussion.

In the cholesteric phase of the propyl homologue, the temperature dependence of the pitch of the helix, albeit over a short temperature range, was measured. In the smectic  $C^*$  phase, the temperature dependence of the spontaneous polarization ( $P_s$ ) and the apparent optical tilt angle ( $\theta$ ) were evaluated.

On cooling the propyl compound from the isotropic liquid, Blue Phases II and I are observed prior to a transition to a cholesteric phase that possesses a left-handed helix (determined from its Grandjean planar texture). On further cooling to 112°C, a change to a non-helical homeotropic nematic phase is observed which shows shear birefringence on mechanical disturbance. At 106°C the phase again becomes helical giving a cholesteric phase which can be identified from its planar texture, but in this case the helix is found to be right-handed. Further cooling results in the formation of a smectic  $C^*$  phase that has a left-hand helix, as determined from its planar pseudo-homeotropic texture. This phase also undergoes a helical twist inversion via a region of infinite pitch to give a right-handed helical smectic  $C^*$  phase at lower temperatures.

Attempts to measure the pitch of the helix in the cholesteric phase of the propyl compound proved to be difficult due to poor alignment of the material. However, the pitch was measured over a short temperature range in the  $Ch_L$  phase using the Cano wedge method<sup>49</sup>; the results are shown in Table XIV. The values obtained show that the pitch increases on decreasing the temperature.

The inversion point for the polarization direction in the ferroelectric phase was determined by a number of different methods. For example, the apparent tilt angle in the ferroelectric smectic  $C^*$  phase was measured from just below the cholesteric to smectic  $C^*$  transition to just above the recrystallisation temperature. The results of these studies are shown graphically in Figure 46. The tilt angle is found to be relatively small close to the transition from the cholesteric phase, however, it increases steadily with decreasing temperature, peaking at a value of 22.5° at 74.6°C. The tilt angle then falls sharply and effectively becomes negative below 62.2°C. When the temperature is held isothermally at 62.2°C, no ferroelectric switching is observed, indicating that the apparent tilt angle is 0°, but this artifact is due to the

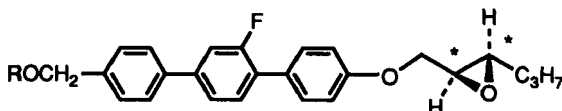


FIGURE 45 Where  $R = C_3H_7$ ,  $C_5H_{11}$  and  $C_7H_{15}$ .

TABLE XIII

Transition temperatures ( $^{\circ}\text{C}$ ) and enthalpies of transition ( $\text{kJ mol}^{-1}$ ) for the 4-((2*S*,3*S*)-3-propyloxiranemethoxy)-2'-fluoro-4''-alkoxymethyl-[1,1':4'',1'']-terphenyls

R	Transition	T( $^{\circ}\text{C}$ )	$\Delta H$ ( $\text{kJ mol}^{-1}$ )
R = C <sub>3</sub> H <sub>7</sub>	Iso - BPII	164.6	
	BPII - BPI	162.9	
	BPI - Ch <sub>L</sub>	158.8	0.67
	m.p.	112.1	
Ch <sub>L</sub> - N <sub>x</sub>	N <sub>x</sub> - Ch <sub>R</sub>	106.3	
	Ch <sub>R</sub> - SmC <sub>L</sub> <sup>*</sup>	103.3	0.48
	(S <sub>C<sub>L</sub></sub> ) - (S <sub>C<sub>x</sub></sub> )	46.8	
	(S <sub>C<sub>x</sub></sub> - (S <sub>C<sub>R</sub></sub> )	46.2	
	m.p.	59	11.4
R = C <sub>5</sub> H <sub>9</sub>	Iso - BPII	137.5	
	BPII - BPI	137.4	
	BPI - Ch <sub>L</sub>	137.3	0.61
	Ch <sub>L</sub> - N <sub>x</sub>	120.1	
	N <sub>x</sub> - Ch <sub>R</sub>	119.9	
	Ch <sub>R</sub> - TGB <sub>A</sub> <sup>*</sup>	118.0	
	TGB <sub>A</sub> <sup>*</sup> - S <sub>A</sub> <sup>*</sup>	117.1	0.34
	S <sub>A</sub> <sup>*</sup> - S <sub>C</sub> <sup>*</sup>	113.1	0.05
	m.p.	39	
R = C <sub>7</sub> H <sub>15</sub>	Iso - BPII	131.3	
	BPII - BPI	130.9	
	BPI - Ch	129.8	0.53
	m.p.	121.9	
Ch - TGB <sub>A</sub> <sup>*</sup>	TGB <sub>A</sub> <sup>*</sup> - S <sub>A</sub> <sup>*</sup>	121.7	0.63
	S <sub>A</sub> <sup>*</sup> - S <sub>C</sub> <sup>*</sup>	115.9	0.06
	m.p.	42	15.9

polarization vanishing and not to the real tilt angle becoming zero. The tilt angle continues to increase, in a negative sense, peaking at a value of  $-22.5^{\circ}$  just above the recrystallisation point. In this study the polarization direction was determined throughout the temperature range of the smectic C<sup>\*</sup> phase. A positive value of the spontaneous polarization, Ps(+), was observed in the smectic C<sub>L</sub><sup>\*</sup> phase, whereas a negative value, Ps(-), was obtained in the lower temperature region of the smectic C<sub>R</sub><sup>\*</sup> phase.

The value of the spontaneous polarization for the propyl compound was determined by using the Diamant bridge method. AC fields were applied using a sine-

TABLE XIV

Temperature dependence (°C) of the pitch (μm) in the cholesteric phase for, 4-((2*S*,3*S*)-3-propyloxiranemethoxy)-2'-fluoro-4"-propoxymethyl-[1,1':4',1'']-terphenyl

Temperature (°C)	Pitch (μm)
124.4	6.69
122.4	7.51
122.0	8.33
122.0	9.87
121.5	10.32

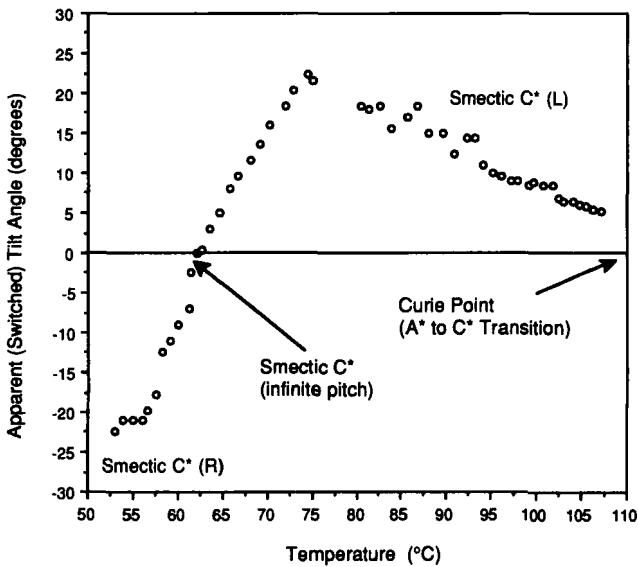


FIGURE 46 The apparent tilt angle (degrees) measured as a function of temperature (°C) for 4-((2*S*,3*S*)-3-propyloxiranemethoxy)-2'-fluoro-4"-propoxymethyl-[1,1':4',1'']-terphenyl.

wave mode and the resulting hysteresis loop was observed on a dual trace oscilloscope with the spontaneous polarization (*P*<sub>s</sub>) being determined accordingly.<sup>50</sup> The polarization was determined using an applied AC voltage of 30 volts (peak to peak) at a frequency of 40 Hz from a temperature just below the smectic *C*<sub>L</sub><sup>\*</sup> to cholesteric *Ch*<sub>R</sub> phase transition. The results obtained are shown in Figure 47. The *P*<sub>s</sub> in the Smectic *C*<sub>L</sub><sup>\*</sup> phase first increases, then decreases with decreasing temperature towards the inversion point. At the inversion temperature, there is a very sharp and discontinuous change in the value of the polarization. At temperatures below this point the polarization becomes negative and begins to increase in magnitude again.

The results show that the helix inverts in the cholesteric phase, and that the helix and the polarization invert at approximately the same temperature in the smectic

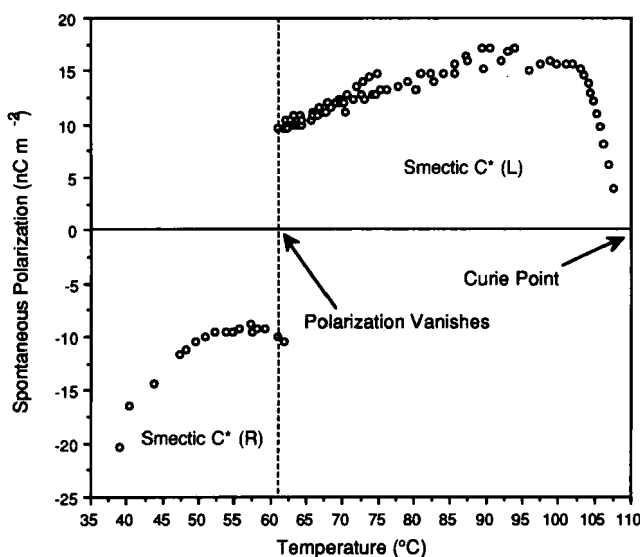


FIGURE 47 Variation in the spontaneous polarization ( $\text{nC cm}^{-2}$ ) as a function of temperature ( $^{\circ}\text{C}$ ) for 4-((2*S*,3*S*)-3-propyloxiranemethoxy-2'-fluoro-4''-propoxymethyl-[1,1':4',1'']-terphenyl.

$\text{C}^*$  phase. Therefore we can use a similar model of competing conformers to explain these results, as we have used previously. In the case of this particular molecular structure, the conformation may be changed by rotation about the  $\text{O}-\text{C1}$  bond, or by rotation about the  $\text{C1}-\text{C2}$  bond. In the first case, unfavourable steric interactions between the  $\text{C1}$  methylene hydrogens and the ortho-aryl hydrogens would give rise to relatively high energy conformations which we can therefore discount. The three lowest energy conformations arising from rotation about the  $\text{C1}-\text{C2}$  bond are shown in Figure 48. Of these, structures (a) and (b) give situations in which the permanent dipoles, and therefore spontaneous polarizations on the macroscopic level, possess opposite signs. The third conformer (c) possesses a higher relative energy due to an unfavourable disposition of the chiral chain relative to the mesogenic core of the molecule, thereby reducing the linearity of the molecule. Preliminary molecular modeling studies have shown that interconversion between the two conformers (a) and (b) is separated by a thermodynamic energy barrier to rotation ( $\Delta E$ ) of approximately  $11.8 \text{ kJ mol}^{-1}$ , which is consistent with the results for rotations about the  $\text{C2}-\text{C3}$  bond in butane.

The properties of this low molar mass liquid crystal are unique, and for the first time an inversion of the helical twist senses in both the cholesteric and chiral smectic  $\text{C}^*$  phases are exhibited. As with the other inversion we suggest that the origin of the crossovers is due to a competition between the distribution of different conformers within the molecule at different temperatures rather than between the relative twisting powers of individual chiral centres. It is also proposed that this distribution can be described in terms of a Boltzmann function. Similar results have also recently been reported on the helix inversion in cholesteric and smectic phases in thin cells.<sup>51</sup>

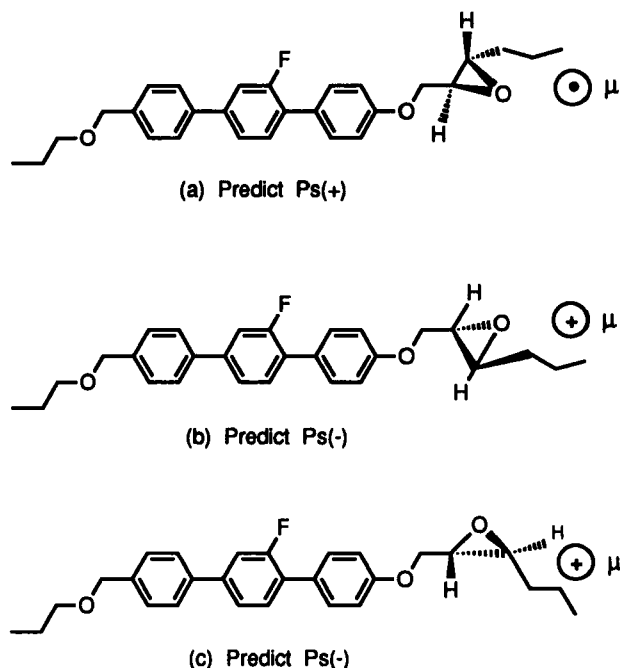
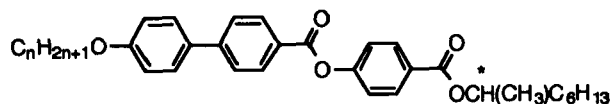


FIGURE 48 Conformational structures produced by rotation about the C1—C2 bond.

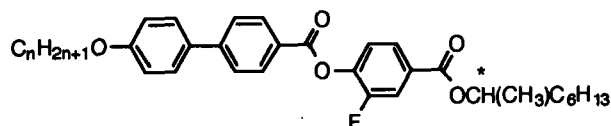
#### 4. ANTIFERROELECTRIC AND FERRIELECTRIC MATERIALS

In the previous sections we have discussed two types of competition which arise because of the chirality of the structures of the molecules. Firstly, we have seen the competition produced between a desire to form helical structures and the need to produce planar layered organizations of the molecules resulting in the formation of frustrated phases. Secondly, we have produced arguments to suggest that there is an internal competition between different chiral conformers in liquid-crystalline systems which can result in the inversion of helical or polarization properties. In the following section, we will describe another form of chiral molecular interaction that results in the minimization of the effects of some macroscopic properties. In particular, we will examine the formation of antiferroelectric phase where the molecules “pair” in order to produce a phase where the spontaneous polarization is reduced to zero in value.

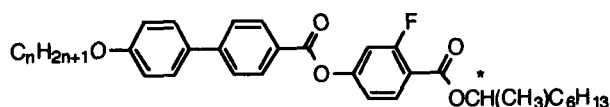
Typically, molecules that exhibit antiferroelectric phases have structures that contain central rigid cores composed of at least three aromatic or heterocyclic rings. Attached to the core is a terminal chiral group that has its chiral centre positioned adjacent to the core, and on the peripheral side of the asymmetric atom there is a chain of at least six carbon atoms in length. Thus, in effect, molecules with this form of structural architecture would be expected to exhibit strong molecular chirality, which might be expected to affect the liquid-crystalline properties of the material.<sup>52</sup> Figure 49 gives a number of examples of homologous series where antiferroelectric phases are found, and transition temperatures are given for in-



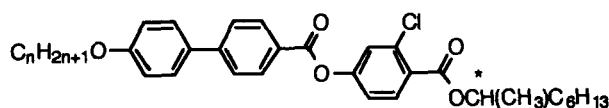
$n = 8$ : Iso - 156 -  $S_A$  - 122 -  $S_{C\alpha}$  - 120.7 -  $S_{C^*}$   
 $S_{C^*}$  - 119 - Ferri - 118 - Anti



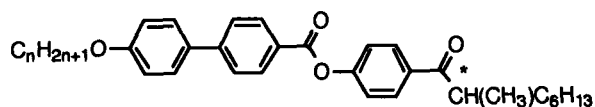
$n = 12$ : Iso - 101  $S_A$  - 80 -  $S_{C^*}$  - 64 - Ferri - 47 - Anti



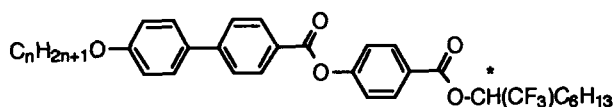
$n = 10$ : Iso - 133 -  $S_A$  - 123 -  $S_{C^*}$  - 118 - Anti



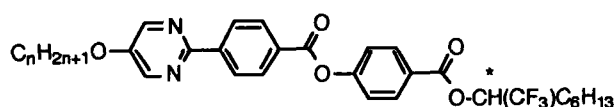
$n = 8$ : Iso - 116 -  $S_A$  - 97 -  $S_{C^*}$  - 95 - Anti



$n = 8$ : Iso - 150 -  $S_A$  - 132 -  $S_{C^*}$  - 60 - Anti



$n = 12$ : Iso - 100 -  $S_A$  - 97 - Anti



$n = 12$ : Iso - 105 -  $S_A$  - 98 - Anti

FIGURE 49 Structures of some homologous series that exhibit antiferroelectric phases.<sup>53</sup>

dividual members. Nearly all of the materials shown have either ester or ketone groups linking the chiral centre to the core; the core can have lateral substituents, and the chiral end group is either 1-methylheptyl or 1-(trifluoromethyl)heptyl.

The number of materials, therefore, that exhibit antiferroelectric and ferroelectric behaviour is limited, and in order to develop structure/property relationships further we synthesized the following homologous series of materials, the (*R*) and (*S*)-1-methylalkyl 4''-(4'-*n*-alkoxybenzoyloxy)biphenyl-4-carboxylates, the general structure of the series which is shown in Figure 50.

The terminal alkoxy and alkyl chains were varied in length and the phase transition types and temperatures were determined. The results obtained are shown in the following three Tables XV, XVI and XVII.

It can be seen from these studies that the antiferroelectric and ferroelectric phases are stabilized as the alkyl chain length (*m*) is extended, with the transition temperatures reaching a maximum for the 1-methylpentyl chiral end group before falling again as the peripheral alkyl chain is increased. It is also interesting to note that there is a very pronounced odd-even effect with respect to the alkyl chain length; in fact the 1-methylbutyl and 1-methylhexyl members do not even appear to exhibit these phases. Similarly, the transition temperatures of the smectic C\* to ferroelectric and ferroelectric to antiferroelectric phase changes rise and reach a maximum (at the dodecyloxy member) before falling again when the alkoxy chain is increased in length from eight to sixteen carbon atoms. These studies also show that these two transitions are very sensitive to optical purity, see Table XVII. The other transitions, liquid to smectic A\*, smectic A\* to smectic C\*, and smectic to crystal J\* do not vary appreciably with optical purity, whereas the transitions to ferro- and antiferro-phases are markedly affected by changes to the enantiomeric excess.

These results seem to show that the molecular chirality is affected by the length of the molecular core (it appears to require at least three aromatic units), and the lengths of the two peripheral aliphatic chains (*n* and *m*), and the location of the chiral centre within the molecule (preferably adjacent to the core), see Figure 51. In essence, the free rotation of the chiral centre is restricted by (a) locating it adjacent to the core and (b) by extending the peripheral aliphatic chain on the external side of the chiral centre; these in turn augment the overall chirality of the system which is affected by the size of the core and the alkoxy chain length. However, as the chains at either end of the molecular structure are extended a point is reached where any further increase in length has little effect on the chirality of the system. Once this limit is passed, extension of the chains results in a dilution of the effects of chirality. This is reflected by the rise in the stability of the antiferro- and ferro-phases as the series are ascended, followed by a leveling-off and then a fall for the higher homologues.

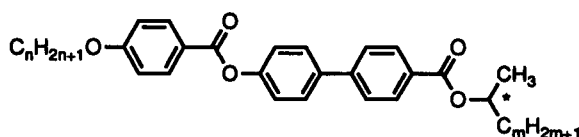


FIGURE 50



TABLE XV

Transition temperatures (°C) and enthalpies of transition (kJ mol<sup>-1</sup>) for the (*R*) and (*S*)-1-methylheptyl 4'-(4'-*n*-alkoxybenzoyloxy)biphenyl-4-carboxylates

n	Abs Conf.	Ps Sign	Helix rotn	Iso to A*	A* to C*	C* to C* <sub>ferri</sub>	C* <sub>ferri</sub> to C* <sub>anti</sub>	Sm to J*	mp
8	S	(+)	<i>l</i>	128.5	[82.1]				91.5
ΔH				5.4	+				27.8
9	S	(+)	<i>l</i>	124.8	99.0	[66]	[62.5]		87.6
ΔH				4.1	+				26.1
10	S	(+)	<i>l</i>	124.5	105.4	75.9	69	[47.8]	65.2
ΔH				5.2					28.4
10	R	(-)	<i>d</i>	124.5	104.9	77.6	72.1	[47.5]	65.7
ΔH				4.9	0.05			4.2	31.7
11	S	(+)	<i>l</i>	120.4	108.4	[69.8]			72.3
ΔH				4.6	0.05				42.7
12	S	(+)	<i>l</i>	118.7	109.0	[77.0]	[68]		78.2
ΔH				3.9	0.13				46.8
13	R	(-)	<i>d</i>	116.1	107.2	70.7			66.7
ΔH				4.0	0.18				45.4
14	R	(-)	<i>d</i>	115.4	109.5	67.2	61	[37]	55.5
ΔH				4.5	0.25				46.4
15	R	(-)	<i>d</i>	112.0	106.6	[45]			59.8
ΔH				4.1	0.25				50.2
16	R	(-)	<i>d</i>	108.9	105.0				66.9
ΔH				4.1	0.23				31.7

Where: [ ] denotes a monotropic phase transition,  
 + denotes an enthalpy too small to be measured.

In order to take this argument concerning rotational freedom of the chiral centre further, the size of the lateral group attached to the chiral centre was varied.<sup>34</sup> It was expected that by increasing the off-axis size of the substituent the free rotation would be suppressed. Thus, the two series of materials shown in Figure 52 were prepared where the value of *p* was changed from 1 to 3 carbon atoms in length. The results for the transition temperatures are shown in Tables XVIII and XIX, respectively.

It can be seen from Tables XVIII and XIX as the size of the lateral group is increased the transition temperatures fall, however, the smectic C\* temperature range is affected more by this process than that of the antiferroelectric phase. Consequently, the antiferroelectric phase is stabilized by the increase in the size of the lateral substituent. This stabilization can be verified by examining the field dependence of the switching in the antiferroelectric phase. For example, the ap-

TABLE XVI

Transition temperatures (°C) and enthalpies of transition (kJ mol<sup>-1</sup>) for the (*R*) and (*S*)-1-methylalkyl 4'-(4'-*n*-decyloxybenzoyloxy)biphenyl-4-carboxylates

CCCCCCCCCOc1ccc(cc1)C(=O)Oc2ccc(cc2)-c3ccc(cc3)C(=O)OC(C)C

m	Abs Conf.	Ps Sign	Helix rotn	Iso to A*	A* to C*	C* to C* <sub>ferri</sub>	C* <sub>ferri</sub> to C* <sub>anti</sub>	Sm to J*	mp
2	S	(+)	<i>l</i>	147.6	111.9			[51.7]	60.6
ΔH				5.3	0.02			3.7	34.7
3	S	(+)	<i>l</i>	137.2	106.3				70.7
ΔH				5.1	0.11				38.9
4	S	(+)	<i>l</i>	135.5	106.5	86.6	74.2	[48.1]	65.6
ΔH				5.4	0.07			4.2	37.2
4	R	(-)	<i>d</i>	133.9	106.7	87.3	85.0	[48.5]	65.7
ΔH				5.8	0.09			4.1	36.8
4	(+/-)			132.4	105.4			[46.1]	65.0
ΔH				5.4	0.16			3.8	33.9
5	S	(+)	<i>l</i>	127.8	104.5			[48.5]	64.85
ΔH				4.4	0.04			3.7	25.1
6	S	(+)	<i>l</i>	124.5	105.4	75.9	69.0	[47.8]	65.2
ΔH				5.2	0.07			3.8	28.4
6	R	(-)	<i>d</i>	124.5	104.9	77.6	72.1	[47.5]	65.7
ΔH				4.9	0.05			4.2	31.7

Where [ ] denotes a monotropic phase transition,  
(+/-) denotes a racemic modification.

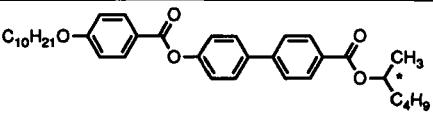
parent tilt angle (or the switching tilt angle) can be measured as a function of the applied electric field at a given temperature in the antiferroelectric phase.

At low fields, because the polarization in the antiferroelectric phase is zero, little or no switching occurs, but at higher fields (greater than the threshold field) the antiferroelectric transforms to a ferroelectric phase and switching occurs normally. Therefore, in the applied field/apparent tilt angle diagram there is a jump in the value of the tilt angle when this occurs. The higher this field is the more stable the antiferroelectric phase is said to be. Figure 53 shows two switching curves for the benzoate series. It can be clearly seen that the threshold for the propyl branch is much higher than that for the ethyl analogue.

A similar conclusion can be drawn from polarization versus applied electric field studies for the ethyl and propyl compounds of both the benzoate and propiolate series. Each material was examined at a temperature just below (0.5°C) its upper transition temperature for the antiferroelectric phase. The polarization versus applied electric field curves were obtained using a Diamant Bridge<sup>50</sup> by applying a sine wave of either 100 or 15 Hz. The propyl substituted compounds were found to show a double hysteresis loop at both frequencies. This hysteresis loop is char-

TABLE XVII

The effect of optical purity—the transition temperatures (°C) and optical purities for the various isomers of 1-methylpentyl 4''-(4'-*n*-decyloxybenzoyloxy)biphenyl-4-carboxylate



Isomer	Iso to A*	A* to C*	C* to C* <sub>ferri</sub>	C* <sub>ferri</sub> to C* <sub>anti</sub>	Sm to J*	[α] <sup>23</sup> <sub>D</sub>	ee(%)
(S)	135.5	106.5	86.6	74.2	48.1	9.5	89.45
(R)	133.9	106.7	87.3	85.0	48.5	9.9	91.1
(+/-)	132.4	105.4			46.1		

Where (+/-) denotes a racemic modification.

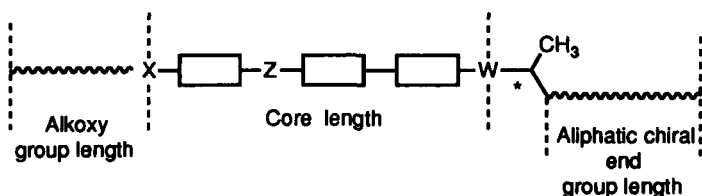


FIGURE 51 General structure of an antiferroelectric material.

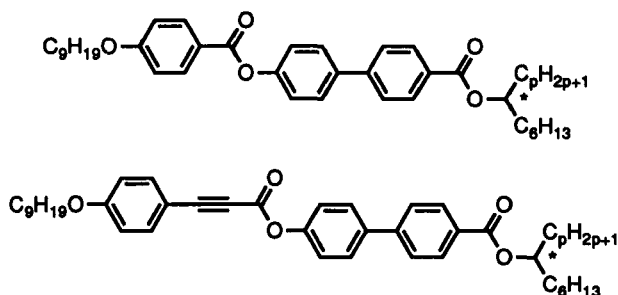


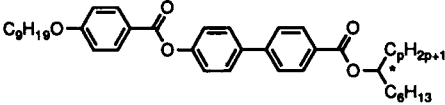
FIGURE 52

acteristic of stable antiferroelectric phases. However, the ethyl substituted compounds exhibit a single hysteresis loop at both frequencies of 100 and 15 Hz. In this context, it has been reported<sup>53</sup> for TFMHPOBC (see Figure 54) that the polarization versus applied electric field hysteresis loop changes from a double loop to a single loop with increasing frequency from 150 Hz to 5 kHz.

It is possible, therefore, that a direct transition from one induced ferroelectric state to the other can occur in an antiferroelectric phase, thereby resulting in the

TABLE XVIII

The transition temperatures (°C) for the (*R*) and (*S*)-1-alkylheptyl 4''-(4'-*n*-nonyloxybenzoyloxy)biphenyl-4-carboxylates

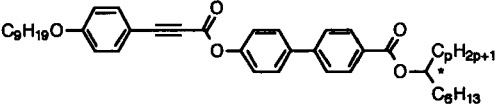


p	Iso to A*	A* to C*	A* or C* to C* <sub>anti</sub>	Recryst
1	119.5	99.4		61.0
2	90.3	64.1	63.9	<RT
3	77.5		50.1	<RT

Where <RT denotes a transition occurring below room temperature.

TABLE XIX

The transition temperatures (°C) for the (*R*) and (*S*)-1-alkylheptyl 4''-(4'-*n*-nonyloxyphenylpropioyloxy)biphenyl-4-carboxylates



p	Iso to A*	A* to C*	A* or C* to C* <sub>anti</sub>	Recryst
1	92.7	65.8		54.0
2	68.9	46.2	45.3	<RT
3	59.8		42.6	<RT

Where <RT denotes a transition occurring below room temperature.

appearance of the single hysteresis loop. Thus, a frequency of 15 Hz may be high enough to produce a direct transition between the two induced ferroelectric states for ethyl substituted materials. Thus, the formation of double hysteresis loops for the propyl homologues indicates that the antiferroelectric structure is greatly stabilized by the introduction of a propyl group at the chiral centre in comparison to that of an ethyl group.

In fact this effect is so pronounced for all of the propyl homologues we have studied that we coined the term the "propyl effect" to describe the enhanced stability of the antiferroelectric phase which reaches a point where it is effectively more stable than the ferroelectric phase.

#### 4.1. A Swallow-tailed Achiral Antiferroelectric Material

Thus, so far chiral compounds of the general type shown in Figure 55 have been found to exhibit unusual properties.<sup>55</sup>

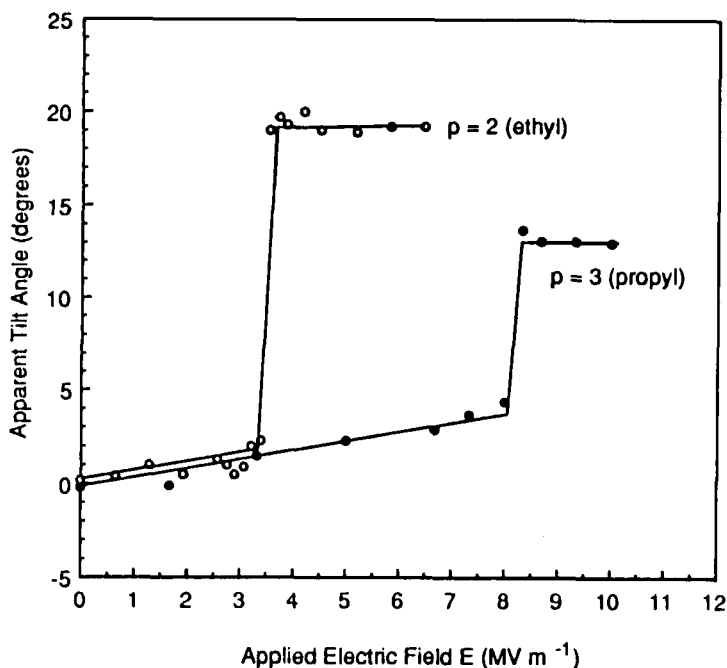


FIGURE 53

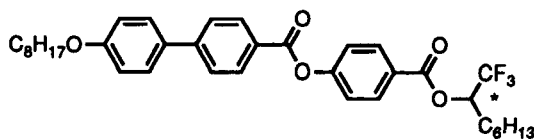


FIGURE 54

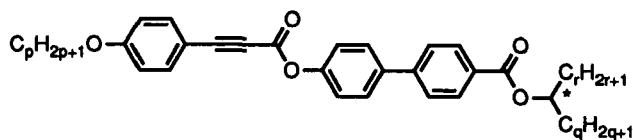


FIGURE 55

We have shown that by independently varying the lengths of the two aliphatic chains, denoted by  $C_qH_{2q+1}$  and  $C_rH_{2r+1}$ , the chirality of the system can be altered. It was found that when the length,  $r$ , of the off-axis alkyl substituent is increased the incidence of antiferroelectric phases also increases. It is suggested that by increasing the alkyl chain lengths,  $q$  and  $r$ , the molecular rotation that occurs about the chiral centre becomes progressively more damped in systems such as the smectic  $C^*$  phase. Moreover, this also increases the chirality and the biaxiality of the system. Taking this kind of study to its ultimate conclusion the length,  $r$ , of the off-axis "lateral" alkyl substituent was increased until it equaled that of the "terminal"

chain length,  $q$ . In doing so a material, 1-propylbutyl 4'-(4''-*n*-nonyloxyphenylpropioloyloxy)biphenyl-4-carboxylate, was synthesized which has no molecular chirality. Its structure is shown in Figure 56.

This material was found to have unusual liquid-crystalline properties in that it did not exhibit a normal smectic C phase, but rather it exhibited a phase that was miscible with the antiferroelectric phases of chiral materials. The transition temperatures of this swallow-tailed compound, determined by thermal optical polarized light microscopy on cooling, are as follows.

I 70.0°C S<sub>A</sub> 54.8 Antiferro 41.7° recryst

The results of differential scanning calorimetry are almost in agreement with microscopic studies and show that this compound exhibits only monotropic liquid-crystalline phases. On heating the material simply melts from the crystal to the isotropic liquid. Cooling shows a transition from the isotropic liquid to the smectic A phase at 70.3°C, further cooling produces two other transitions, first to the antiferroelectric phase, at 54.8°C, and then to a complex crystal form at 45.9°C. The values measured for the enthalpies of transition are given in Table XX.

The data shows that the smectic A to antiferroelectric phase change is first order in nature, and clearly this observation is not consistent with the transition being from a smectic A to a smectic C phase, which in the vast majority of cases is second order. Actually, the first order phase change is more in keeping with a transition from a smectic A to a more ordered phase such as an antiferroelectric or smectic I/F phase where the molecules are still tilted with respect to the layer planes.

Confirmation that this material exhibits an antiferroelectric phase was achieved through several different miscibility studies, Figure 57 shows one example of such phase diagrams. The antiferroelectric phase of the test material proved to be continuously miscible with the antiferroelectric phase of the standard. The smectic C\* phase was found to disappear as the percentage of the test compound in the binary

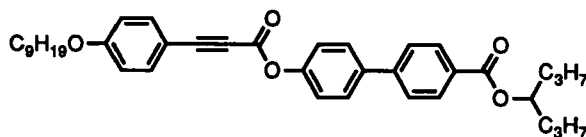


FIGURE 56

TABLE XX

Enthalpies of the transitions (kJ mol<sup>-1</sup>) for the swallow-tailed compound 1-propylpropyl 4'-(4''-*n*-nonyloxyphenylpropioloyloxy)biphenyl-4-carboxylate

Transition	Enthalpy (kJ mol <sup>-1</sup> )
Cryst to Iso	44.5
Iso to S <sub>A</sub>	3.1
S <sub>A</sub> to Antiferro.	0.7
Antiferro to Cryst	18.9

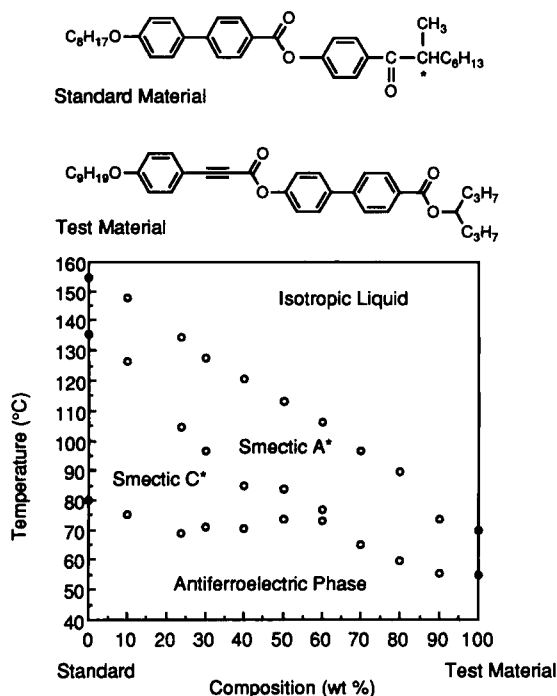


FIGURE 57 Miscibility phase diagram for mixtures (wt.%) of (*S*)-4-(2-methyloctanoyl)phenyl 4'-*n*-octyloxybiphenyl-4-carboxylate (standard) and the test material 1-propylpropyl 4'-(4''-*n*-nonyloxyphenylpropyloxy)biphenyl-4-carboxylate.

mixtures rose above 60% by weight, thus indicating that the test material does not exhibit a smectic C\*/C phase. As with other miscibility studies the smectic A phase was found to be continuously miscible across the full concentration range. As this phase diagram shows that the antiferroelectric phases of both materials are miscible, it is reasonable to conclude, therefore, that the antiferro-phase of the test material has a similar structure to that of a true antiferroelectric phase even though it is not chiral. If this is the case then this material is a novel example of a non-chiral low molar mass compound exhibiting an "antiferroelectric-like" phase.

With this particular study we appear to have come full circle. Much of the work reported has been focused on rotational trapping as a way of increasing the relative chirality of a system. In another way this has the effect of subtly broadening the molecular structure, so that the inclination to form mesophases is reduced, but not suppressed totally. In a sense, therefore, by broadening the molecular structure we may have unduly increased the local biaxial ordering (over a few molecules at most). Thus, we appear to have induced antiferroelectric order without the need for chirality. The major question posed by this study concerns how the molecules self-organize to form a zigzag layer packing. One approach is to consider the dimeric associations of the molecules, because it has been suggested previously that dimers with bent structures favour antiferroelectric ordering.

Most materials which exhibit antiferroelectric behaviour have asymmetric structures, with high optical purities, leading to physical properties and behaviour that

are strongly dependent on chirality.<sup>56,57</sup> However, it has been shown recently that antiferroelectric phases can occur in racemic mixtures as well,<sup>58,59</sup> thereby shedding doubt on the postulation that antiferroelectric behaviour is dependent on the “degree of chirality” of the system. Moreover, it has also been discovered that some non-chiral main chain polymers exhibit antiferroelectric ordering in the smectic C phase. Consequently, it is possible that the antiferroelectric order arises because of the zigzag conformation shape of the main chain structure.<sup>60</sup> Similar zigzag structures can be obtained from dimers<sup>61</sup> of the type shown in Figure 58. In this dimer, the molecules have a bridging chain that has an odd number of methylene links. When the linking chain is in its all trans conformation, it causes the two aromatic units to be tilted in opposite directions to each other with respect to the layer normal. Thus, a “bent dimer” is produced which when packed with other dimers together (see Figure 59(c)) leads to a zigzag layer structure which is similar to that obtained for an antiferroelectric phase.

For pairing in chiral systems, the molecules will have fairly strong dipoles which act along the  $C_2$  axis of the layer structure. This results in the material having a high value for the spontaneous polarization for an individual layer. Conversely, pairing of the molecules will have the favourable effect of compensating for the strong lateral dipoles along the  $C_2$  axis thereby reducing the value of the polarization, as shown in Figure 59(a). Thus, there will be a competition between the need to reduce the overall polarity of the system (i.e., to lower the spontaneous polarization) and the need to preserve a layer structure where the molecules are tilted. The result of this competition is that the molecules in adjacent layers tilt in opposite directions thereby preserving the local layer structure yet at the same time

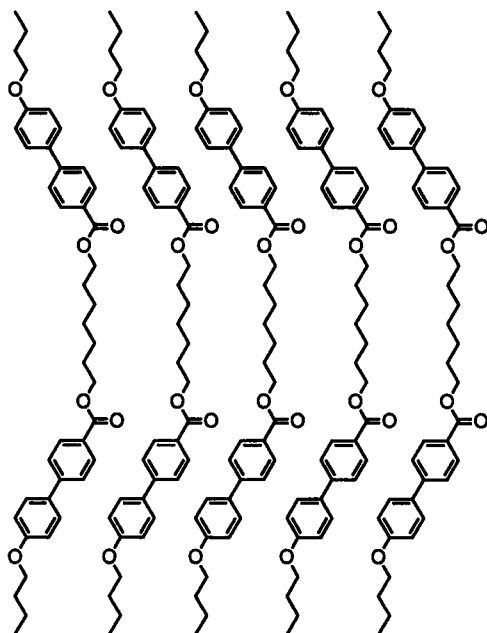


FIGURE 58 Proposed zigzag structure for dimers.



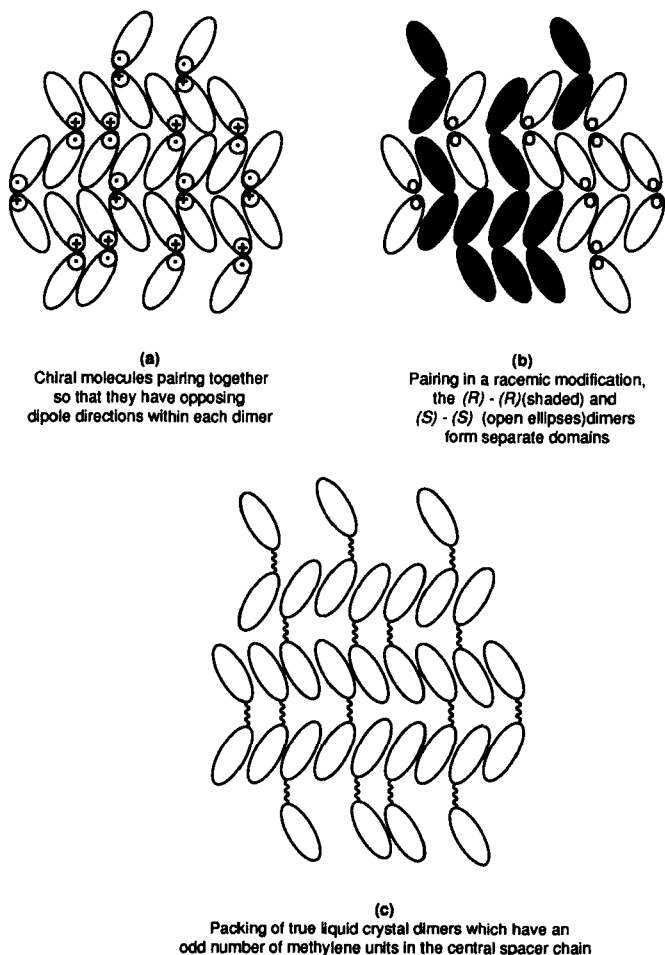


FIGURE 59 Packing of molecules producing zigzag structure.

compensating for the layer polarization. In the case of racemic modifications a similar effect is suggested to be present. However, because of the differences in the packing of *(R)*-*(S)* dimers with respect to the *(R)*-*(R)* and *(S)*-*(S)* dimer ordering, it is thought that like-chiral-molecules aggregate together to give an inhomogeneous distribution of *(S)*-*(S)* and *(R)*-*(R)* pairs. The resulting phase, therefore, has an antiferroelectric structure, as shown in Figure 59(b).<sup>62</sup>

In the case of the swallow-tailed compound, the forked branch point in the terminal chain is formed through the bonding of an  $sp^3$  hybridized carbon atom. Therefore, the forked-tail of the molecule is no longer co-planar with the molecular core, but bent at an angle with respect to the long axis. The bending of the swallow tail would be expected to cause the formation of either bent or zigzag shaped dimers through the interleaving of the terminal chains between layers. As a consequence, the packing of bent shaped dimeric species could result in the formation

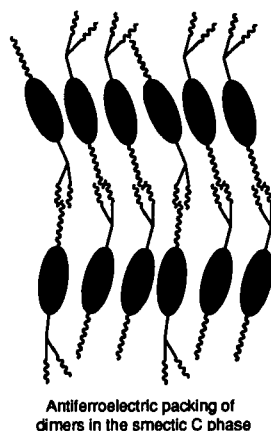


FIGURE 60 Antiferroelectric packing of dimers for the swallow-tailed compound.

### Effect of Molecular Chirality on TGB Phases

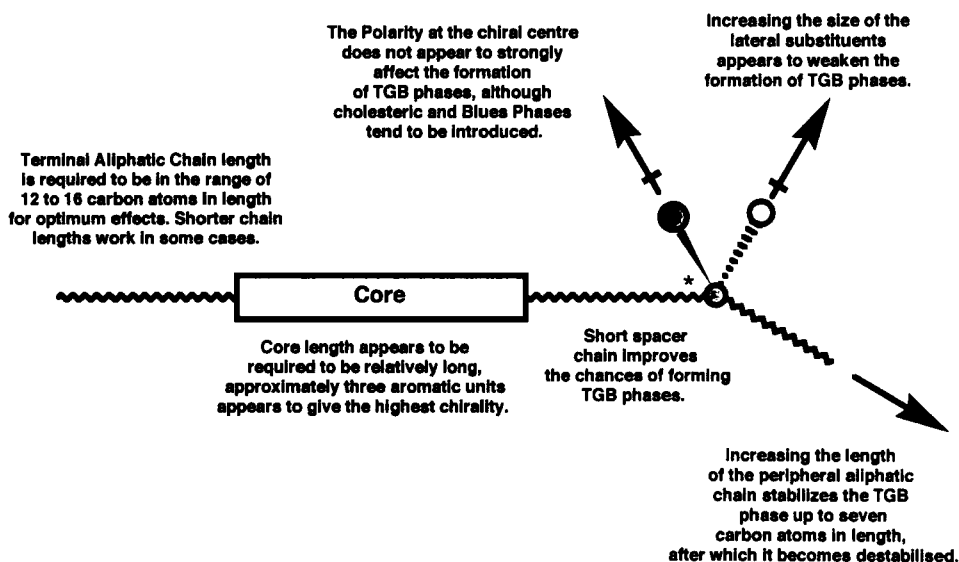


FIGURE 61

of tilted phases and in particular the formation of antiferroelectric structures, as shown in Figure 60.

## 5. CONCLUDING REMARKS

This investigation into chirality is still ongoing, however, the large number of materials that have been prepared and the structure/property correlations that have

## Effect of Molecular Chirality on Inversion Phenomenon

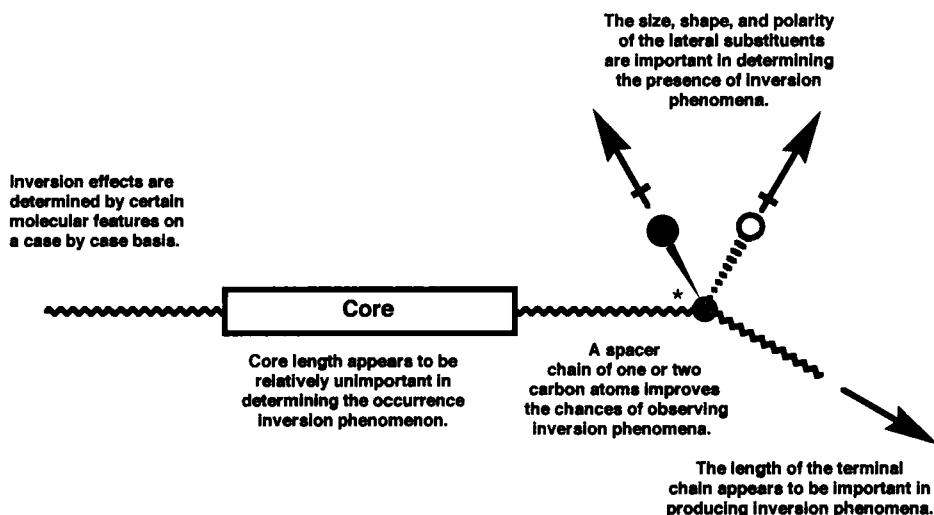


FIGURE 62

## Effect of Molecular Chirality on Antiferroelectric Phases

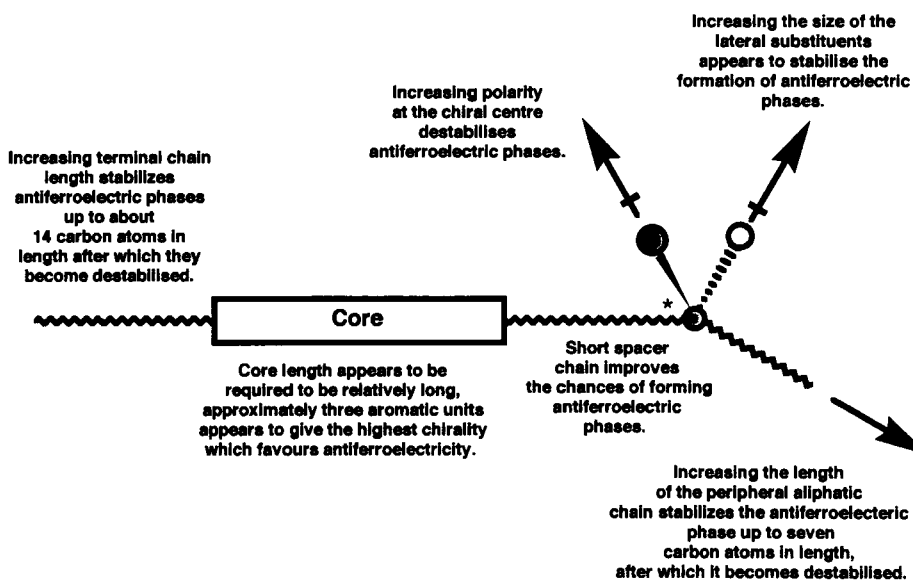


FIGURE 63

been developed from results on their liquid crystal properties are extensive. In this article we have been only able to draw upon a few examples of the relationships that we have examined. However, rather than summarise again in words the relationships between phase structure/properties and molecular structure that we have

developed in the main text, we offer the following three figures (based on Figure 13) which attempt to crystallise our main observations. Figure 61 shows the relationship between molecular chirality and TGB phases, Figure 62 the relationship between molecular chirality and inversion phenomena, and lastly Figure 63 which depicts the effects of molecular structure on antiferroelectric phases.

## Acknowledgment

We would like to acknowledge the support of the Science and Engineering Research Council (SERC) (Dr. A. J. Slaney), the SERC and the Ministry of Defence (Dr. C. J. Booth), ERASMUS (Mr. J. D. Vuijk), Nippon Mining (Dr. I. Nishiyama) and BNR/Thorn EMI (industrial lectureship for Dr. P. Styring). We are also grateful to Dr. M. A. Waugh and E. Chin of AT&T Bell Laboratories for their help in the synthesis of materials, Mr. A. Roberts, Mrs. B. Worthington, and Mr. R. Knight of the School of Chemistry, Hull for their invaluable help with the spectroscopic analysis of intermediates and final materials.

## References

1. See for example *Chemical Reviews*, special issue on Enantioselective Synthesis, **92**, 739–1140, (1992) and articles therein.
2. J. W. Goodby, *J. Mater. Chem.*, **1**, 307 (1991).
3. P. P. Crooker, *Liq. Cryst.*, **5**, 751 (1989).
4. S. R. Renn and T. C. Lubensky, *Phys. Rev. A*, **38**, 2132 (1988).
5. A. M. Glass, J. S. Patel, J. W. Goodby, D. H. Olson and J. M. Geary, *J. Appl. Phys.*, **60**, 2778 (1986); A. M. Glass, J. W. Goodby, D. H. Olson and J. S. Patel, *Phys. Rev. A*, **38**, 1673 (1988).
6. N. Hiji, A. D. L. Chandani, S. Nishiyama, Y. Ouchi, H. Takezoe and A. Fukuda, *Ferroelectrics*, **85**, 99 (1988); K. Furukawa, K. Terashima, M. Ichiashi, S. Saitoh, M. Miyazawa and T. Inukai, *Ferroelectrics*, **85**, 63 (1988).
7. R. S. Cahn, C. K. Ingold and V. Perlog, *Angew. Chem. Int. Ed.*, **5**, 385 (1966).
8. R. S. Cahn and C. K. Ingold, *J. Chem. Soc.*, 612 (1951).
9. G. Solladie and R. G. Zimmermann, *Angew. Chem. Int. Ed. Engl.*, **24**, 64 (1985); *J. Org. Chem.*, **50**, 4062 (1985); R. Ch. Geivandov, I. V. Goncharova and V. V. Titov, *Mol. Cryst. Liq. Cryst.*, **166**, 101 (1989).
10. J. Budau, R. Pindak, S. C. Davey and J. W. Goodby, *J. Phys. (Paris) Lett.*, **45**, L-1053 (1984); C. J. Booth, G. W. Gray, K. J. Toyne and J. P. Hardy, *Mol. Cryst. Liq. Cryst.*, **210**, 31 (1992); Zhong-Li, B. M. Fung, R. J. Tveig, K. Betterton, D. M. Walba, R. F. Shao and N. A. Clark, *Mol. Cryst. Liq. Cryst.*, **199**, 379 (1991).
11. R. B. Meyer, *Mol. Cryst. Liq. Cryst.*, **40**, 33 (1977).
12. S. Garoff and R. B. Meyer, *Phys. Rev. Lett.*, **38**, 848 (1977).
13. C. H. Bahr and G. Heppke, *Phys. Rev. A. Rapid Commun.*, **37**, 3179 (1988).
14. H. R. Brand, P. E. Cladis and P. L. Finn, *Phys. Rev. A*, **31**, 361 (1985).
15. A. J. Leadbetter in "Thermotropic Liquid Crystals," (Ed. G. W. Gray), Critical Reports on Applied Chemistry, Vol. 22, Wiley and Son, Chichester, 1987, pp. 1–27.
16. D. M. Walba, M. B. Ros, N. A. Clark, R. Shao, K. M. Johnson, J. Y. Liu and D. Doroski, *Mol. Cryst. Liq. Cryst.*, **198**, 51 (1991).
17. J. W. Goodby, E. Chin, T. M. Leslie, J. M. Geary and J. S. Patel, *J. Am. Chem. Soc.*, **108**, 4729 (1986); J. W. Goodby and E. Chin, *J. Am. Chem. Soc.*, **108**, 4736 (1986); D. M. Walba, S. C. Slater, W. N. Thurmes, N. A. Clark, M. A. Hondscho and F. Supon, *J. Am. Chem. Soc.*, **108**, 5210 (1986).
18. K. Yoshimo, M. Ozaki, T. Sakurai, M. Honma and K. Sakamoto, *Jpn. J. Appl. Phys.*, **23**, L175 (1984).
19. D. M. Walba, S. C. Slater, W. N. Thurmes, N. A. Clark, M. Handschy and F. Supon, *J. Am. Chem. Soc.*, **108**, 5210 (1986).
20. J. W. Goodby, J. S. Patel and E. Chin, *J. Phys. Chem.*, **91**, 515 (1987).
21. A. J. Slaney and J. W. Goodby, *J. Mater. Chem.*, **1**, 5 (1989).

22. P. G. de Gennes, *Solid State Commun.*, **10**, 753 (1972).
23. A. A. Abrikosov, *Z. Eksp. Teor. Fiz.*, **32**, 1442 (1957); *Soviet Phys., JETP*, **3**, 1174 (1957).
24. S. R. Renn and T. C. Lubensky, *Mol. Cryst. Liq. Cryst.*, **209**, 349 (1991).
25. G. Strajer, R. Pindak, M. A. Waugh, J. W. Goodby and J. S. Patel, *Phys. Rev. Lett.*, **64**, 1545 (1990).
26. J. W. Goodby, M. A. Waugh, S. M. Stein, E. Chin, R. Pindak and J. S. Patel, *J. Am. Chem. Soc.*, **40**, 4153 (1989); *Nature*, **337**, 449 (1989).
27. K. J. Ihn, J. Zasadzinski, R. Pindak, J. S. Patel and J. W. Goodby, Proc. of the 49th Ann. Conf. of Elec. Micro. Soc. USA (1991); *Science*, **258**, 275 (1992).
28. A. J. Slaney, PhD Thesis, Hull University (1992); I. Nishiyama, PhD Thesis, Hull University (1992); J. D. Vuijk, MSc Thesis, Hull University (1991); C. J. Booth unpublished results.
29. A. Bouchta, H. T. Nguyen, M. F. Achard, F. Hardouin, C. Destrade, R. J. Twieg, A. Maaroufi and N. Isaert, *Liq. Cryst.*, **12**, 575 (1992); H. T. Nguyen, R. J. Twieg, M. F. Nabor, N. Isaert and C. Destrade to be published in *Ferroelectrics*; C. J. Booth, K. T. Toyne and J. W. Goodby, unpublished results; J. W. Goodby, M. A. Waugh, S. M. Stein, E. Chin, R. Pindak and J. S. Patel, *J. Am. Chem. Soc.*, **111**, 8119 (1989).
30. Ya. S. Freidxon, Ye. G. Tropsha, V. V. Tsukruk, V. V. Shilov, V. P. Shibaev and Yu. S. Lipatov, *J. Polym. Chem. (USSR)*, **29**, 1371 (1987).
31. E. C. Bolton, P. J. Smith, D. Lacey and J. W. Goodby, *Liq. Cryst.*, **12**, 305 (1992).
32. G. Scherowsky, A. Schliva, J. Springer, K. Kuhnpast and W. Trapp, *Liq. Cryst.*, **5**, 1281 (1989).
33. D. R. Nelson, *Phys. Rev. Lett.*, **60**, 1973 (1988); P. L. Gemmel, D. J. Bishop, G. J. Dolan, J. R. Kwo, C. A. Murray, L. F. Schneemeyer and J. Waszczak, *Phys. Rev. Lett.*, **59**, 2592 (1987).
34. I. Nishiyama, PhD Thesis, University of Hull (1992).
35. A. Yoshizawa, I. Nishiyama, M. Fukumasa, T. Hirai and M. Yamane, *Jpn. J. Appl. Phys.*, **28**, L1269 (1989).
36. A. J. Slaney, PhD Thesis, Hull University (1992).
37. Y. Sato, T. Tanaka and K. Kubota, Abst. 17th Jpn. Liq. Cryst. Conf. (Ekisho-Tohronkai, Sapporo, 1991) P. 268.
38. A. J. Slaney and J. W. Goodby, *Liq. Cryst.*, **9**, 849 (1991).
39. J. W. Goodby, E. Chin, J. M. Geary and J. S. Patel, in "Proc. 11th Int. Liq. Cryst. Conf., Berkeley, USA, June 1986, FE-030 (Abst); J. S. Patel and J. W. Goodby, *Phil. Mag. Lett.*, **137**, 91 (1987).
40. N. Mikami, R. Higuchi, T. Sakurai, M. Ozaki and Y. Yoshimo, *Jpn. J. Appl. Phys.*, **25**, L833, 1986.
41. J. S. Patel (unpublished results).
42. J. W. Goodby, E. Chin, J. M. Geary, J. S. Patel and P. L. Finn, *J. Chem. Soc. Faraday Trans., I*, **83**, 3429 (1987).
43. G. W. Gray and D. G. McDonnell, *Mol. Cryst. Liq. Cryst. Lett.*, **34**, 211 (1977).
44. J. W. Goodby and T. M. Leslie, *Mol. Cryst. Liq. Cryst.*, **110**, 175 (1984).
45. A. J. Slaney, I. Nishiyama, P. Styring and J. W. Goodby, *J. Mater. Chem.*, **2**, 805 (1992).
46. A. J. Slaney, PhD Thesis, University of Hull (1992).
47. P. Styring, J. D. Vuijk, A. J. Slaney, I. Nishiyama and J. W. Goodby, *J. Mater. Chem.*, **3**, 399, (1993).
48. J. G. Hill, K. B. Sharpless, C. M. Exon and R. Regenye, *Organic Synthesis*, **63**, 66 (1984).
49. F. Cano, *Bull. Soc. Fr. Mineral*, **91**, 20 (1968); F. Grandjean, *Compt. Rend. Acad. Sci.*, **172**, 71 (1921); P. R. Gerber, *Z. Naturforsch.*, **359**, 619 (1980).
50. H. Diamant, K. Drenck and R. Pepinsky, *Rev. Sci. Instr.*, **28**, 30 (1957).
51. I. Dierking, F. Giebelmann, P. Zugenmaier, W. Kuczynski, S. T. Lagerwall and B. Stebler, *Liq. Cryst.*, **13**, 45 (1993).
52. J. W. Goodby and E. Chin, *Liq. Cryst.*, **3**, 1245 (1988).
53. J. Lee, *et al.*, *Jpn. J. Appl. Phys.*, **29**, L1122 (1990); I. Nishiyama, J. W. Goodby and E. Chin, *J. Mater. Chem.*, in press; K. Furukawa, K. Terashima, M. Ichihashi, S. Saitoh, K. Miyazawa and T. Inukai, *Ferroelectrics*, **85**, 63 (1988); A. Yoshizawa, *et al.*, *Jpn. J. Appl. Phys.*, **28**, L1269 (1989); Y. Suzuki, T. Hagiwara, Ikawamura, N. Okamura, Y. Imai, Y. Ouchi, T. Kitazume, M. Kakimoto, H. Takezoe and A. Fukuda, *Liq. Cryst.*, **6**, 167 (1989); I. Nishiyama, A. Yoshizawa, M. Fukumasa and T. Hirai, *Jpn. J. Appl. Phys.*, **28**, L2248 (1989); S. Inui, S. Kawano, M. Saito, H. Iwane, Y. Takanishi, K. Hiraoka, Y. Ouchi, H. Takezoe and A. Fukuda, *Jpn. J. Appl. Phys.*, **987** (1990).
54. H. Orihara, T. Fujukawa, Y. Ishibashi, Y. Yamada, N. Yamamoto, K. Mori, K. Nakamura, Y. Suzuki, T. Hagiwara and I. Kawamura, *Jpn. J. Appl. Phys.*, **29**, L333 (1990).
55. I. Nishiyama and J. W. Goodby, *J. Mater. Chem.*, **2**, 1015 (1992).
56. J. W. Goodby and E. Chin, *Liq. Cryst.*, **3**, 1245 (1988).
57. A. D. L. Chandari, Y. Ouchi, H. Takezoe and A. Fukuda, *Jpn. J. Appl. Phys.*, **27**, L276 (1988).

- 58. H. Takezoe, J. Lee, A. D. L. Chandani, E. Gorecka, Y. Ouchi, A. Fukuda, K. Terashima and F. Furukawa, *Ferroelectrics*, **114**, 187 (1991).
- 59. Y. Yamada, K. Mori, N. Yamamoto, H. Hayashi, K. Nakamura, M. Yamawaki, H. Orihara and Y. Ishibashi, *Jpn. J. Appl. Phys.*, **28**, L1606 (1989).
- 60. J. Watanabe and M. Hayashi, *Macromolecules*, **22**, 4083 (1989).
- 61. Y. Takarishi, H. Takezoe, A. Fukuda, H. Komura and J. Watanabe, *J. Mater. Chem.*, **2**, 71 (1992).
- 62. Y. Takanishi, K. Hiraoka, V. K. Agrawal, H. Takezoe, A. Fukuda and M. Matsushita, *Jpn. J. Appl. Phys.*, **30**, 2023 (1991).